Progress in Materials Science 109 (2020) 100635

Contents lists available at ScienceDirect

Progress in Materials Science

journal homepage: www.elsevier.com/locate/pmatsci

Metal oxides based electrochemical pH sensors: Current progress and future perspectives

Libu Manjakkal[a], Dorota Szwagierczak[b], Ravinder Dahiya[a,*]

[a] Bendable Electronics and Sensing Technologies (BEST) Group, James Watt School of Engineering, University of Glasgow, G12 8QQ Glasgow, UK
[b] Institute of Electron Technology, Krakow Division, Zablocie 39, 30-701 Krakow, Poland

ARTICLE INFO

Keywords:
Electrochemical pH sensor
Metal oxide
Potentiometric sensor
ISFET
Flexible sensors

ABSTRACT

Electrochemical pH sensors are on high demand in numerous applications such as food processing, health monitoring, agriculture and nuclear sectors, and water quality monitoring etc., owing to their fast response (< 10 s), wide pH sensing range (2–12), superior sensitivity (close to Nernstian response of 59.12 mV/pH), easy integration on wearable/flexible substrates, excellent biocompatibility and low cost of fabrication. This article presents an in-depth review of the wide range of MOx materials that have been utilized to develop pH sensors, based on various mechanisms (e.g. potentiometric, conductimetric, chemi-resistors, ion sensitive field effect transistor (ISFET) and extended-gate field effect transistor etc.). The tools and techniques such as potentiometric and electrochemical impedance spectroscopic that are commonly adopted to characterize these metal oxide-based pH sensors are also discussed in detail. Concerning materials and design of sensors for various practical application, the major challenges are toxicity of materials, interfernce of other ions or analytes, cost, and flexibility of materials. In this regard, this review also discusses the metal oxide-based composite sensing (active) material, designs of pH sensors and their applications in flexible/wearable biosensors for medical application are examined to present their suitability for these futuristic applications.

1. Introduction

Ion sensitive metal oxides (MO_x) with micro- and nanostructured morphologies have gained increasing interest with potential applications in electrochemical-biomedical sciences and across numerous other scientific disciplines. Their unique electrical, electrochemical and biocompatible properties assert their utility in the fabrication of sensors for applications such as water and food quality monitoring, wearable systems for chronic diseases and industrial applications. With high surface to volume ratio, the MO_x enhances the sensitivity, selectivity and catalytic activity. Further, the fast response and long lifetime in different environmental conditions, make MO_x excellent candidates for the next generation of wireless sensing and online monitoring applications. Among various sensors used in these applications, the development of electrochemical pH sensors is one of the major implementations of MO_x. The centrality of pH in a wide range of fields including chemistry, agriculture, food processing, pharmaceuticals, environmental science, chemical and biomedical engineering applications [1–8] also brings MO_x to the forefront of materials research. The measurement and control of hydrogen ion concentration, represented in terms of pH value, is essential for many chemical and biological reactions. The pH value can greatly influence the physiological, biological and medical state of a person [9–14]. For example, the pH at chronic wound sites changes from slightly acidic (pH 5.5) for a healthy skin to basic (pH 7.0–8.5) for wounded skin due to the

* Corresponding author.
E-mail address: Ravinder.Dahiya@glasgow.ac.uk (R. Dahiya).

https://doi.org/10.1016/j.pmatsci.2019.100635
Received 2 February 2019; Received in revised form 7 May 2019; Accepted 10 December 2019
Available online 16 December 2019

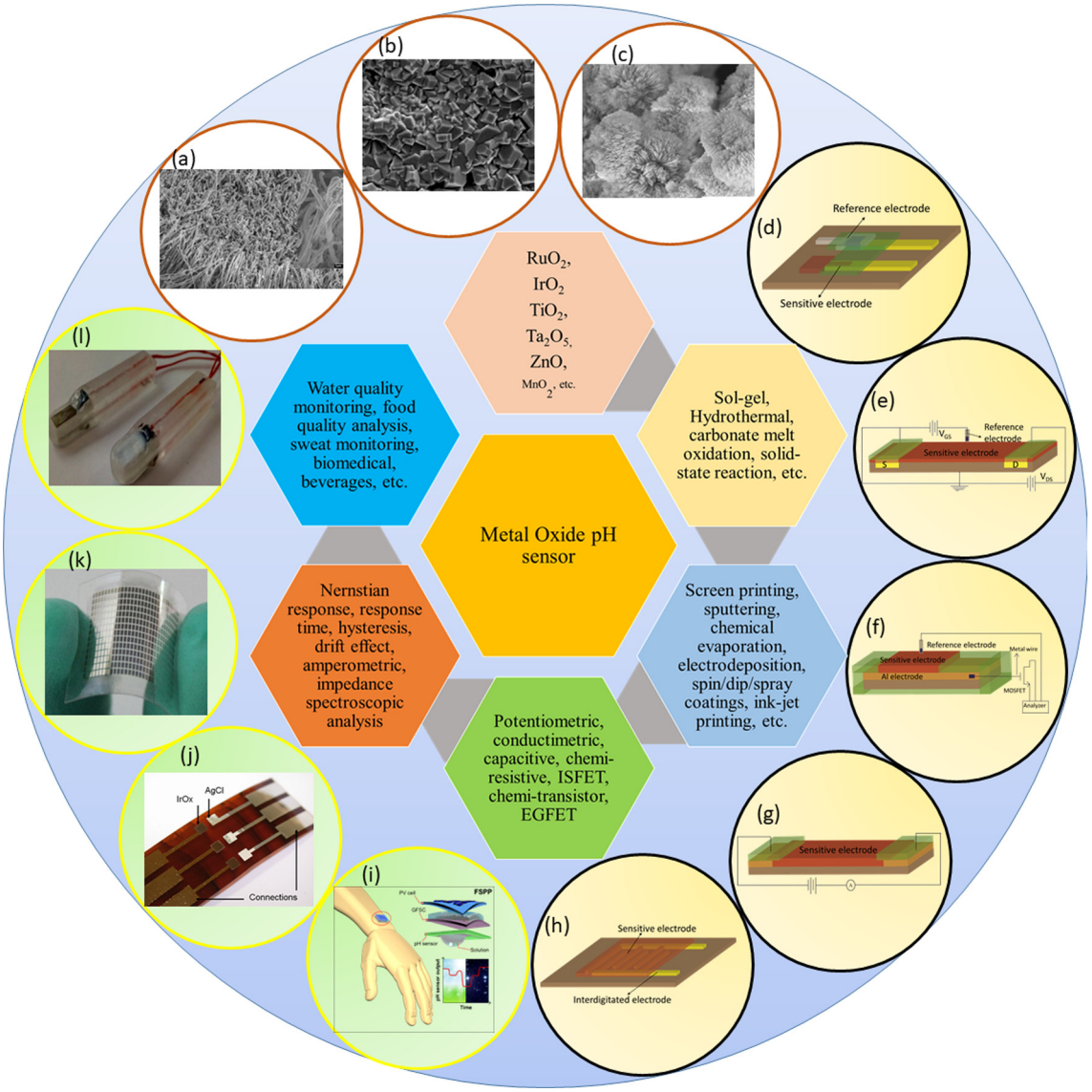

Fig. 1. Various metal oxide based pH sensors – key methods for preparation of electrode materials and sensor fabrication, type of sensors, parameters for analysis and applications: (a) structural properties of few materials "*Reprinted from Publication* [38] *with permission from Elsevier*". (b) "*Reprinted from Publication* [39] *with permission from Elsevier*", (c) "*Reprinted from Publication* [25] *with permission from Elsevier*" (d)–(h) different types of pH sensors including potentiometric, chemi-resistive, ISFET, EGFET and interdigitated, and (j)–(l) applications of pH sensors werable and food quality monitoring (i) *with permission* [3]. (j) "*Reprinted from Publication* [40] *with permission from Elsevier*". (k) *with permission* [41], (l) "*Reprinted from Publication* [42] *with permission from Elsevier*".

presence of bacterial colonies and enzymes [1]. Regular monitoring of pH value of skin can be helpful in terms of detecting the pathogenesis of skin diseases such as irritant contact dermatitis, acne vulgaris, atopic dermatitis, etc. [4,5,15]. Various cellular processes and enzymatic reactions in the human body also depend on the pH value. Likewise, in food processing, the pH value carries the signature of protein denaturization, gelification, growth and mortality of microorganisms and the germination or inactivation of bacteria spores [16–19]. Furthermore, water pollution and industrial wastewater can be effectively monitored by measuring the pH value [2,20–22]. In water pollution determination, a stable measured pH in the range of 6.5 to 8.5 is essential to ensure good quality.

The advances in pH sensing technology have focussed on enhancing the sensitivity, operational life time, biocompatibility, rapid response in wider ranges of pH, cost-effectiveness and portability etc by using proper sensitive materials. Several MO_X materials have been reported recently for the development of pH sensors in pollution monitoring [22–24], biological and food quality applications [10,16] as well as emerging application areas such as flexible and wearable systems [1,3,4,25–30]. Fig. 1 shows some examples of recently developed pH sensors based on MOx which are integral to our daily life. Considering that several parameters govern the performance of a pH sensor, and the emergence of MO_x as key material for the development of these sensors, the systematic review of

the MO_x based pH sensor presented here will be helpful for further progresses in terms of fabrication and applications. In particular, it is crucial to investigate the ionic exchange between sensitive nanomaterial and electrolyte. The variation in ionic concentration and the pH value of a solution, significantly change the electrochemical properties including electrochemical potential, impedance and capacitance of the electrodes. In addition, the influence of microstructure, particle shape, size and surface morphology of MO_x nanostructures (e.g. thin films, nanotubes, nanobelts, nanowires, nanorectangles, nanorods, etc., shown in Fig. 1a–c) on the electrochemical properties etc. are presented. Few review articles have discussed the state-of-art of research and progress in pH sensing so far with limited discussion. For example, Korostynska et al. [31] have discussed the development of polymer-based pH sensors and Yuqing et al. [32] have presented new technologies for the detection of pH. Likewise, Qin et al. [33] have reviewed the developments in microfabricated electrochemical pH sensors, including those for free chlorine sensors. Recently Alam et al. [34] have pointed out the importance of polymers and organic materials-based pH sensors for healthcare applications. Some review papers on MO_x based sensors have also been published and these include the one by Voanu and Guth [35], where the solid-state pH electrodes using MO_x have been discussed. The pH sensing performance and properties of metal-MO_x and MO_x based pH sensors are described by Glab et al. [36]. The ion exchange sensing mechanisms of MO_x pH sensors have been reviewed by Kurzweil [37]. The discussions in these review papers are limited to different materials and designs of pH sensors (Fig. 1d–h), the comparative study of fabrication methods and the sensing mechanisms. A substantial discussion is needed on different classes of pH sensitive MOx materials, to provide an accelerative impact on the research and development of novel miniaturized pH sensors for real-time monitoring in extreme high temperature/pressure and aggressive chemical environments, as well as for flexible/wearable applications (Fig. 1i–l). In this review article, we address these gaps and present a comprehensive and perspective analysis of electrochemical MO_x based pH sensors. The elaborate discussion in this review includes various materials and types of pH sensors, and the analysis of sensing mechanism with different detection techniques including electrochemical impedance spectroscopy (EIS) analysis for material investigations.

This review is organized as follows: Section 2 briefly compares major types of electrochemical pH sensors and highlights the case for MO_x based sensors. Various detection techniques and categories of MO_x pH sensors such as potentiometric, conductimetric/chemi-resistors, ion sensitive field effect transistors (ISFET) and extended-gate field effect transistors (EGFET) are presented in Section 3. Iimportant characteristics of pH sensors are mentioned in Section 4. In Section 5 we provide the sensing mechanism of MO_x based pH sensors. The detailed description and comparison of various pH sensitive MO_x materials in terms of fabrication, merits/demerits, performance and applications are described in Section 6. In Section 7, we discuss the challenges and future prospects of MO_x pH sensors including their applications in food processing, pollution monitoring, wearable/flexible systems and extreme environments. Finally, the conclusions are summarized in Section 8.

2. Electrochemical pH sensors

The past few decades have witnessed a considerable effort in terms of the development of electrochemical (potentiometric, conductimetric, capacitive, and resistive) and non-electrochemical (including calorimetric and optical) pH sensors [30,43–51] for various applications. The sensitive electrodes (SE) which is a major component of any electrochemical pH sensor are mainly based on the glass membrane electrodes, MO_x, metal/MO_x, polymers and carbon. A comparison of SEs from these materials (Fig. 2) shows that ion sensitive MO_x based on micro and nano structures received great interest. Electrochemical methods are the most widely adopted techniques for pH sensing. Many materials and designs have been investigated for the development of SEs for such sensors. The advantages and disadvantages of the most popular SEs implemented for the fabrication of electrochemical pH sensors are compared in Fig. 2. It is evident from Fig. 3 that the conventional glass based sensors have been popular for the pH measurement. However, mechanical fragility and the lack of flexibility/bendability hinder their implementations in emerging areas such as wearable systems. Further, durability and performance instability at high temperatures and pressures limit their use for pollution monitoring and other industrial applications. These drawbacks of glass-based sensors have encouraged researchers to explore alternative ways in pH sensing. Among these, MO_x based pH sensors have attracted significant attention due to their high sensitivity (close to Nernstian response), fast response time (< 10 s), long life time (> 1 year), ease of miniaturization, stability in different atmospheres and biocompatibility of majority of MO_x.

3. Metal oxide based pH sensors and detection techniques

The significance of MO_x as sensitive electrodes for pH sensors fabrication and their sensing mechanisms was first highlighted by Fog and Buck [52]. Until now, various MO_x have been used for the fabrication of pH sensors, among which Pt-group oxides, such as RuO_2 and IrO_2, have recieved the greatest attention owing to their remarkable sensitivity to hydrogen ions and high degree of accuracy. There are only few reports which utilized PtO_2 as a pH sensor. According to Fog and Buck [52], the PtO_2 based pH sensor shows a sensitivity of 46.7 mV/pH in the range 2–12 and hysteresis effect for pH 2-12-2 loop is $\pm$ 100 mV. Furthermore, certain other transition MO_x, perovskite materials and mixed oxides such as Ta_2O_5, TiO_2, SnO_2, CeO_2, WO_3, Bi_2O_3-Nb_2O_5, PbO_2, IrO_2-TiO_2, RuO_2-TiO_2, perovskite lithium lanthanum titanate (LLTO), yttria stabilized zirconia (YSZ), molybdenum oxide bronzes, etc. are investigated for pH sensor applications (discussed in following sections). In addition to this, some works have been done in the area of metal/ MO_x based pH sensors such as those based on antimony and bismuth and the redox equilibrium between the metal/MO_x phases (e.g. Sb-Sb_2O_3) attributes to the origin of their pH sensitivity [36,37,53,54]. However, the performance of such systems in pH measuring is limited because they are undesirably sensitive to several redox agents and exhibit a systematic deviation from the expected behavior. To overcome these issues, many efforts have focused on the deisgn of thin and thick MO_x films on the top of non-conductive substrates and studying their suitability for a wide range of applications.

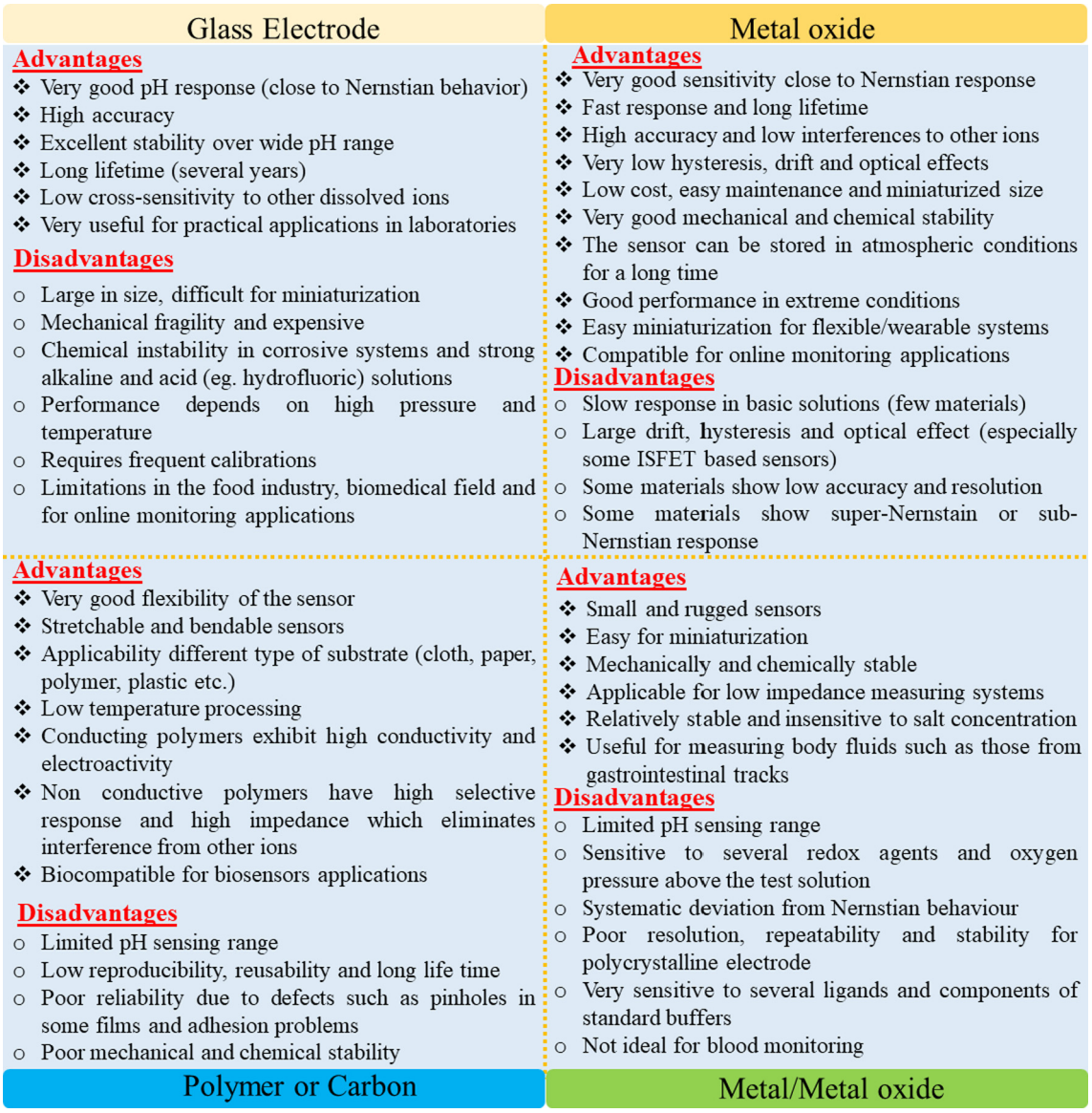

Fig. 2. Comparison of the major materials used for electrochemical pH sensor fabrication.

The sensitivity of the MO_x pH sensor significantly depends on the type of material composition (Section 6 describes different types of MO_x) and the deposition method since both these factors could influence the microstructure, porosity, surface homogeneity and crystalline structure of the material. This leads to variation in sensitivity of electrodes. Generally, the sensitivity of the pH sensors is expressed in terms of Nernstian response. If the sensitivity factor lies close to the ideal Nernstian response (59.14 mV/pH at 25 °C derived from the Nernst equation), the sensor is expected to show excellent performance. Fig. 3 summarizes various MOx based SEs which show sensitivity factors close to the ideal Nernstian response. We investigated the sensitivity of different MO_x including IrO_2 [40,52,55–57], RuO_2 [22,52,58–60], TiO_2 [52,61–64], SnO_2 [52,65–68], Ta_2O_5 [52,69–71], WO_3 [72–76] and ZnO [77–81] and compared with the theoretical sensitivity at 25 °C derived from the Nernst equation (59.14 mV/pH), as shown in Fig. 3a. Fig. 3b represents the variation in sensitivity of the sensors of different materials fabricated by screen printing [22,23,59,60,82], sputtering [58,64,65,71], sol-gel [40,61,83–85] and electrodeposition [56,57,72] methods. In addition to this, the fabrication steps and mode of operation leads MO_x based SEs into a different class of electrochemical pH sensors as discussed in the following section.

MO_x based pH sensors are mainly categorized as: potentiometric, conductimetric/inductive/capacitive, chemi-resistive and ISFETs [33,86–88] or transistors based sensors [33,89,90]. In this section along with different types of pH sensors, we describe major techniques used to understand their working mechanisms such as potentiometry, cyclic voltammetry [37,84,91] and EIS [38,69,70,92–96].

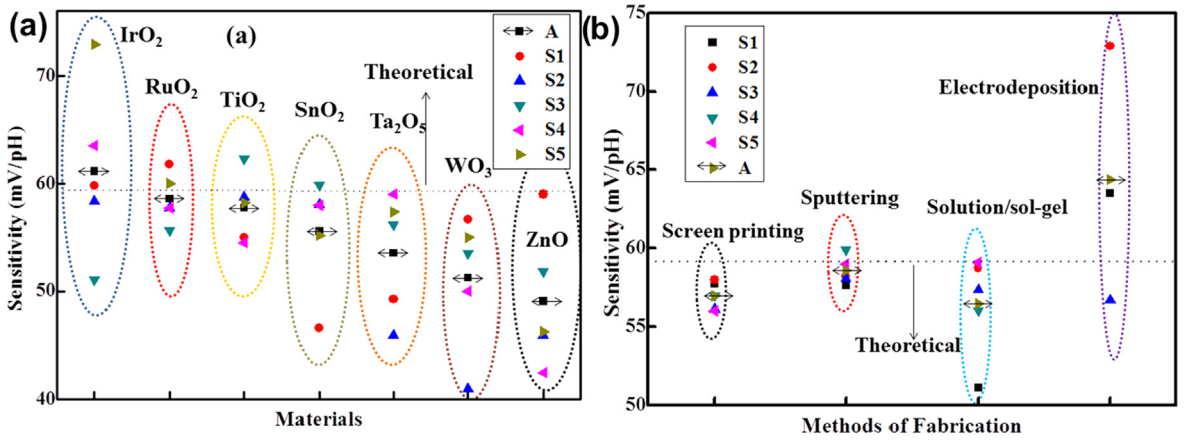

Fig. 3. Comparison of potentiometric pH sensitivity of different MOx materials fabricated using different methods and comparison with the theoretical slope of Nernst relationship - variation of sensitivity with (a) materials and (b) methods of fabrication (A- average sensitivity, S1-sample #1, S2 sample #2, S3-sample #3, S4- ample #4 and S5-sample #5).

3.1. Potentiometric pH sensor

Most of the reported pH sensors working based on potentiometric method. For this method, the sensor consists of a combination of a sensitive electrode and a reference electrode for which glass-based pH electrode is a major example. Thin and thick films of MO_x in the form of nanostructures (nanowire, nanotube, nanoflower, etc.), have been used as SEs. Considering the ease of fabrication, miniaturization as well as precise and reliable operation, thick film based potentiometric sensors fabricated by screen printing method are commonly used for measuring the pH of a solution [1,2,22,60,97]. This method has the advantage that both the SE and the RE can be deposited on the same substrate. A schematic representation of a screen-printed potentiometric pH sensor is shown in Fig. 4a. In potentiometric pH sensors, Ag/AgCl is one of the most commonly used RE for a stable potential [37,97–100]. Even though different MO_x have been considered (Section 6) as SE, one of the major disadvantages of potentiometric pH sensors, especially in context with miniaturized devices for wireless applications, is the lack of a suitable RE. To overcome this issue, researchers have recently proposed thick film technology for fabrication of Ag/AgCl RE [54,99–103]. Thick film RE on an alumina substrate, reported by Cranny et al. [104] uses various Ag/AgCl pastes for the electrode fabrication. These include polymer Ag/AgCl, glassy AgCl and glassy Ag/AgCl. These electrodes show high Cl^- ion sensitivity which is very close to the theoretical Nernstian behavior. Sun and Wang [105] reported the fabrication of RE (with Cl^- ion sensitivity of 54.7 mV/decade) by low cost and simple electroless deposition and electroplating techniques which can be used for mass production of disposable devices. The lack of potential stability during long-term operation (instability of AgCl layer causes decomposition over time) and cross-sensitivity in testing solutions due to the absence of KCl layer are some crucial drawbacks of the majority of proposed thin and thick film REs. In our work, we proposed a novel lead-free glass-KCl composite based layer in order to stabilize the potential at the RE. For the RE fabrication, sodium hypochlorite solution was used to chloridize a part of the Ag conductive layer and thereby to form AgCl. Glass composite-KCl paste was printed on the top of AgCl which stabilized Cl^- concentration in the RE [60,97]. A schematic of the developed thick film RE on an alumina substrate is shown in Fig. 4b. As compared to glass based REs, the fabricated thick film RE showed a potential of 10 mV and measured lifetime over 2 years [97]. We have also realized the fabrication of RE on alumina and low temperature co-fired ceramic (LTCC) substrates for potentiometric pH sensor [23,101,102]. Following the above approach, we also developed flexible RE suitable for flexible sensing devices [103].

Sensitivity in potentiometric based sensors is determined by the potential difference between RE and SE immersed in a solution of unknown pH using Nernstian relation. The slope of the Nernstian relationship predicts the sensitivity of the sensors for a RuO_2 based pH sensor as shown in Fig. 4c. The observed slope factor 56 mV/pH conveys its high sensitivity (close to ideal Nernstian response). Response time, stability, selectivity, interference of other ions and non-ideal effects such as hysteresis and drift are major characteristics of a potentiometric thick film pH sensor that are discussed in Section 4. The excellent performance of the potentiometric pH sensors has received promising attraction for online monitoring application. For example, RuO_2 based pH sensors are successfully implemented for online water quality monitoring. In the aspect of online water quality monitoring, MO_x based low cost miniaturized pH sensors developed using screen printing technology are promising as this technology offers numerous advantages, such as integration of SE, RE and electronic circuits for wireless transmission in a single module or in a three dimensional stack [23,106,107]. In addition to this, wearable sensors based on potentiometric method offer high selectivity and quick response to the variation of pH of body fluids including sweat, tear or wound fluid making such sensors suitable for healthcare system applications [108].

3.2. Capacitive/conductimetric/inductive based pH sensor

A capacitive/inductive/conductimetric pH sensor exploits changes in electrical properties such as capacitance or impedance of a film deposited on interdigitated electrodes (IDE) in response to the electrochemical reaction occurring at the solution-SE interface.

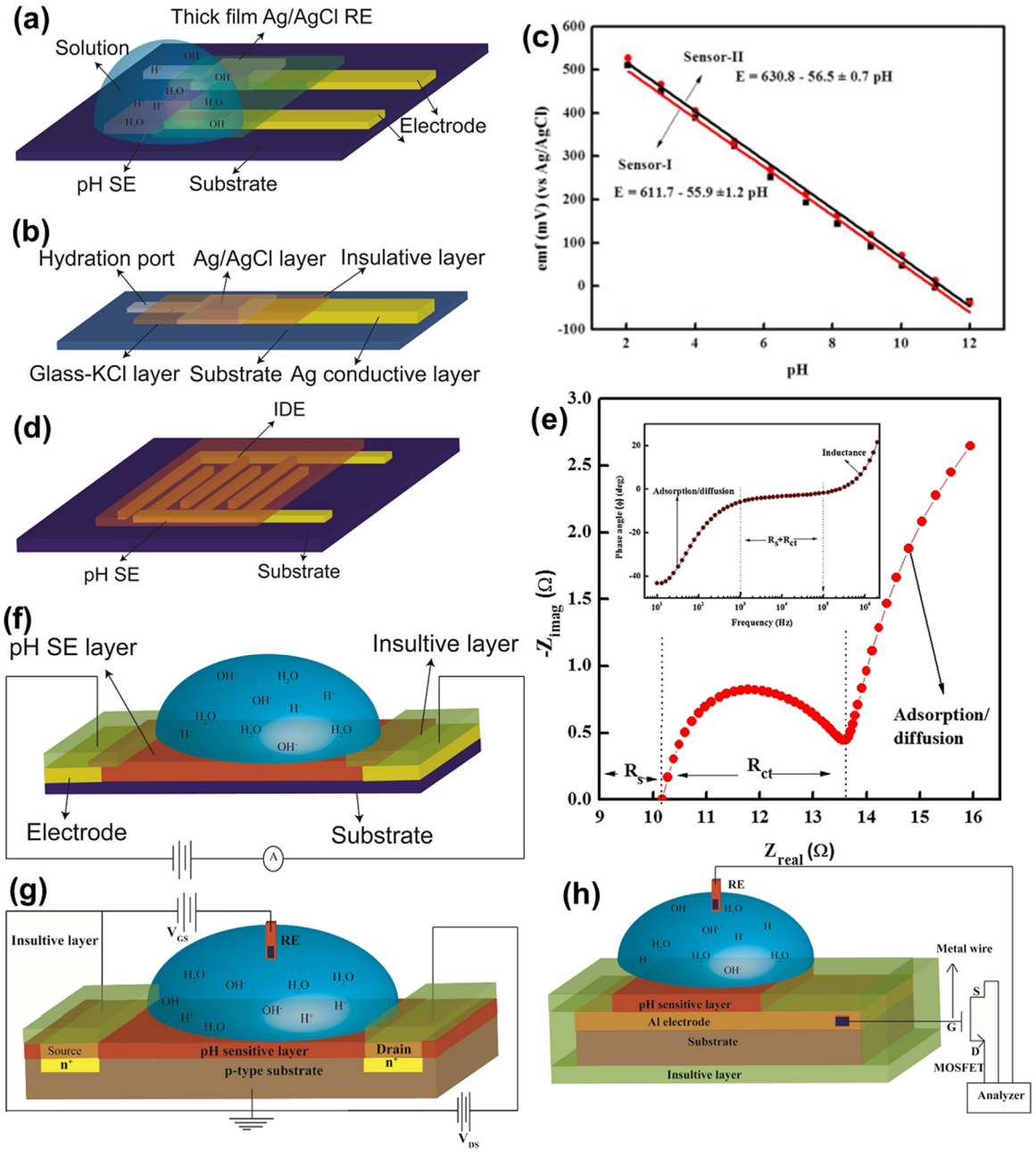

Fig. 4. (a) Schematic representation of potentiometric pH sensor. (b) Schematic representation of thick film Ag/AgCl RE (c) Nernstian response of RuO_2 based pH sensor, *"Reprinted from Publication* [102] *with permission from Elsevier"*. (d) Schematic representation of IDE based conductimetric pH sensor, (e) EIS analysis representing the Nyquist plot and Bode plot (inset) of RuO_2 based thick film pH sensor for ion exchange and charge transfer "*Reprinted from Publication* [93] *with permission from Elsevier"*. Schematic representation of a (f) chemi-resistor (g) ISFET and (h) EGFET (with measurement setup) based pH sensors respectively.

The majority of conductimetric pH sensors have IDE structure and operate without RE [31,92–94,109–111]. A planar IDE based sensor is a simple two electrode probe configuration of an electrochemical cell setup and is widely used for miniaturized applications of sensors, transducers and actuators [92,109,112–116]. The conductimetric method is easy and less expensive as compared to any other method. As shown in Fig. 4d, the fabrication of conductimetric/capacitive pH sensors is simple and cheaper than any other method involving two basic steps - deposition of IDE on a substrate and deposition of the sensitive layer. Screen printing has been widely used for depositing the conducting electrode and the SE on the substrate [31,69,93,109,111]. IDE based structure allows mass production of sensors with miniaturized size, well defined geometry, compactness and sensitivity. Even though this type of sensor has several advantages, due to the possible degradation by long-term operation in different biological and chemical conditions, its

applications are limited. Moreover, the conductivity of solution has a significant influence on the sensing performance of MO_x based conductimetric sensors [69,101]. Polymer based conductimetric sensors have been widely used for biomedical applications [31]. The electrochemical reaction at MO_x- solution interface of an IDE based pH sensors can be investigated by using EIS analysis.

The EIS analysis is a non-destructive steady-state method and is used for analyzing a complex electrochemical system over a broad range of frequencies for sensors, batteries and supercapacitors [3,92,117–121]. This technique enables measuring the response of a circuit or an electrochemical system and is useful in elucidation of the sensing mechanism of a MO_x pH sensor by getting insight into phenomena, such as adsorption, ion exchange, charge transfer, diffusion, etc. [38,70,92,93,96,119,120]. One of the best designs of a sensor with two electrodes configurations for EIS analysis is the one with an IDE structure [92,109]. In impedance spectroscopic data analysis, the features of an investigated system can be portrayed by using Nyquist and Bode plots (Fig. 4e). These plots are useful to analyze conventional electric circuits and the equivalent circuits to describe electrochemical properties of the electrodes and their interaction with a solution. The Bode plot reveals the capacitive, resistive and inductive features of the electrochemical system. In most of the electrode-solution interface reactions, the variation in impedance of a Faradaic reaction may be due to (1) adsorption of reacting species (2) diffusion of ions or (3) both adsorption and diffusion processes together [119–121]. In addition to Faradaic reaction, electrochemical double layer (*edl*) may also develop during-electrode-solution reaction. These phenomena may be related to the contribution of electrolyte, the electrode-solution interface, the nature of the material and electrochemical reaction occurring on the electrode. In our work, we observed from the EIS analysis of IDE based pH sensors that the sensing mechanism of thick film RuO_2 based pH sensors can be attributed to a combination of electron transfer and ion exchange processes at the solution/MO_x interface as illustrated in Fig. 4e. In the high-frequency range, the conductivity and charge transfer processes depend on the solution and sensing layer properties are dominant. However, in the low-frequency range, ion exchange (adsorption/diffusion) processes prevail and sensor characteristic strongly depends on the solution pH. The ion exchange processes also depend on the material properties, like structure, composition, porosity and surface homogeneity [92,93].

3.3. Chemi-resistive/Conductimetric pH sensor

The chemi-resistor and conductimetric based MO_x pH sensors work by similar principle and they do not require a RE for their operation. In chemi-resistor pH sensors, the SE deposited between the two conducting electrodes is shown in Fig. 4f. The pH sensitive semiconductor nanomaterials are mainly used for fabrication of chemi-resistor pH sensors. In this type of pH sensors, the change in H_3O^+/OH^- ions in the solution generates a change in electrical properties, in particular changes in resistance and conductance of the SE material [33]. The sensing performance of a chemi-resistor based pH sensor is strongly dependent on the degree of protonation. There are only few reports on chemi-resistive based pH sensor with MO_x as SE [122]. It was found that for TiO_2 nanowires (NW) based chemi-resistive pH sensor with increasing pH from acidic to basic, the conductance value deceases linearly with a resolution of 5.68 ± 0.28 nS/pH [123]. The decrease in conductance is due to the reduction and increases in the depletion layer at the surface of the TiO_2 NWs from reacting with H^+/OH^- ions. For operating the chemi-resistive sensors, an external power supply is often required. To overcome the need for bulky power sources, we have reported a CuO based self-powered flexible chemi-resistive pH sensor. For this self-powered application, a flexible solar cell was used as an energy generator and a flexible graphene foam based supercapacitor was applied as an energy storage device [3]. In addition to the MO_x, there are few other reports on graphene and CNTs based chemi-resistor pH sensors [89,90].

3.4. Ion-sensitive field effect transistor (ISFET) pH sensor

ISFET is a type of potentiometric device which operates similarly to metal oxide field effect semiconductor transistor (MOSFET) [124] (shown in Fig. 4g). In 1970, Bergveld [88] used the first ISFET for measurements of ion activities in electrochemical and biological environments. In ISFET, the gate is covered with an ion-sensitive layer and is placed between the source and drain (Fig. 4g). The current flowing between source and drain is controlled by the electrostatic field generated by the gate. In this method, instead of measuring the potential difference between the two sides of the glass membrane, the current passing through the transistor is recorded. The wide range of materials used for making ion-sensitive layers on a gate includes ceramics, organics, polymers or catalytic metal layers [33,68,71,87,88,124]. The pH sensing mechanism of the oxide surface of a gate electrode can be described by the site binding theory [125]. A detailed review of ISFETs as pH and biosensors is beyond the scope of this article as it has been made available previously, for example those by Nakazato [126] and Lee et al. [127].

ISFETs can be easily adapted to a broad range of chemical, biomedical and biochemical measurements [28,124] and as compared with glass pH sensor, they have many advantages including miniaturized size, low cost, and fast response. Since ISFETs are directly formed on the FET electrode, they also have several disadvantages such as device instability, low current sensitivity and sensitivity to light, etc. [33]. The optical effect, hysteresis, and drift are the three non-ideal characteristics observed in ISFET based pH sensors. To overcome these drawbacks, Spiegel et al. [128] introduced EGFET, where FET is isolated from the chemical solution as the sensitive film is deposited at the end of signal line extended from the FET electrode [129,130], as illustrated in Fig. 4h. EGFETs are widely used for biosensor applications [128–132] and their major advantages are long-term stability, insensitivity to light and temperature drift, and disposability. The pH sensing mechanism of EGFET can be described by site binding theory. Only few semiconductor MO_x (e.g. SnO_2 on FTO substrate [133], ITO [134]) were utilized for EGFET based pH sensor fabrication [135,136]. In addition to ISFET and EGFET, recently there are many reports on the fabrication of chemi-transistor and electrolyte gated field effect transistor (ElGFET) and reparative extended gate ion-sensitive field-effect transistor (SEGISFET) based pH sensors [137]. Organic semiconductors are mainly used for the development of chemi-transistor and EGFETs based pH sensors [33]. Qin et al. [33] recently reported a detailed

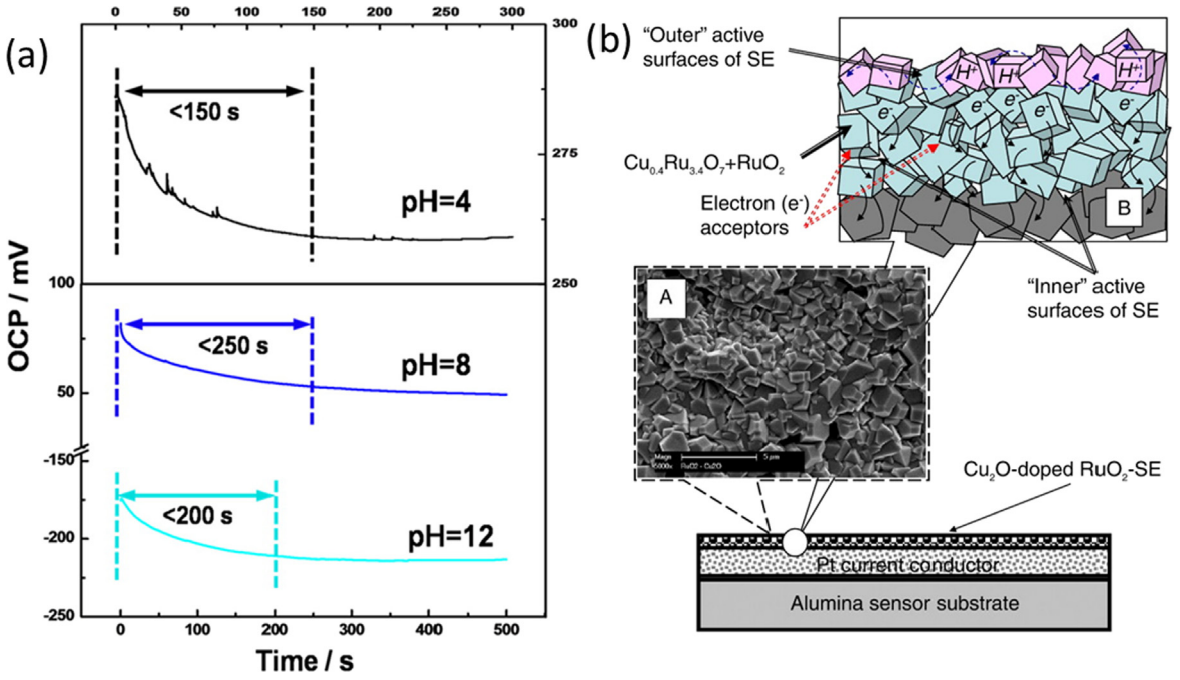

Fig. 5. The response time curves of IrO_2-rGO based sensor in buffer solution at different pH value"*Reprinted (adapted) with permission from* [138] *Copyright (2016) American Chemical Society"*. (b) A cross-sectional view of the Cu_2O doped RuO_2 SE on substrate (A) SEM image of surface of SE (B) tortuous paths of charge carriers to the Pt current conductor "*Reprinted from Publication* [39] *with permission from Elsevier"*

comparative study of the structure and operating mechanism of such type micro-fabricated electrochemical pH sensors.

4. Characteristics of pH sensor

The performance of the pH sensor is determined by their response time, stability, selectivity, interference of other ions and non-ideal effects such as hysteresis and drift. These characteristics, which depend on many parameters, of the metal oxide-based pH sensor is discussed in the following sections.

4.1. Response time

The response time of a solid state potentiometric pH sensor is defined as the time (t_{90}) required for its open circuit potential (*ocp*) or electromotive force (*emf*) to reach 90% of an equilibrium value after immersing the sensor in the solution of a given pH value [38]. In order to analyze the response time of the sensor, the pH value is drastically changed from the acidic to the basic solution and vice versa, and the output potential is measured. The response time of a MO_x pH sensor depends on many factors related to the SEs, including the composition, structural properties, morphology, thickness, and pore size. The response time of the sensor also depends on measurement range of pH value. Most of the sensors show a faster response time in the acidic region as compared to alkaline solution. As an example, potential–time curves of IrO_2-rGO based sensor in buffer solution at different pH value are shown in Fig. 5a [138]. At an acidic pH of 4, the sensor shows faster response time (150 s) than the sensor in a basic solution of pH value 12 (200 s). In any case, the response of the sensor in neutral pH region is much slower than in both the acidic and basic regions [138]. In comparison to acidic and basic solutions, the fastest response of the sensor in acidic solutions is related to ion exchange of small mobile H^+ ions, dominant in acidic solutions. In our previous work on RuO_2-Ta_2O_5 based sensor, we also have observed that in the acidic region of solution, the sensor exhibited a much shorter response time (< 8 s), than in basic solutions (< 15 s). This faster response is related to H^+ diffusion which is dominant in acidic solutions [23].

The method of fabrication changes the morphologies and surface properties of materials, which also influences the response time of pH sensors. As an example, Zhuiykov et al. [39] observed that, for planar thick film Cu_2O doped RuO_2 SEs, the response time to pH changes was strongly dependent on the electrode thickness, decreasing from ~80 to 120 s for a SE thickness of ~2 μm to ~25 s for a thickness of ~5 μm [39]. These changes in response time are due to the surface electrochemical reaction associated with the grain size and grain faceting of the SE present in the "inner" active surfaces of the SE (shown in Fig. 5b), and the increase in open porosity with increasing thickness. When a solution reacts on this surface of the MO_X layer, three complex interfaces will be formed (i) outer surface:- the MOx SE/solution macro-boundaries (ii) inner surface:- the MOx SE/solution micro-boundaries due to penetration of the ions in the liquid into pores and inter-grain regions and (iii) the oxide SE layer/support Pt layer interface. For the faster response of the sensor, the first two regions are very significant. The ions from the outer active surface are diffused or adsorbed into the inner

active surfaces. To further investigate the surface morphologies of SE impact on response time, Zhuiykov et al. [39] compared the crystalline properties of thin and thick film SE. The thicker film presented higher porosity and larger grain size (1.5–2 μm) than the thin film (grain size 600 to 800 nm). The dimension of the inner active region of thick film is in the range of 50–110 nm. For this SE, the thicker film had presented faster response due to the well crystallized material.

Similarly, Xu and Zhang [38] found that the response time is less than 40 s for the pH sensitive electrodes based on RuO_2 nanoparticles modified with vertically aligned carbon nanotubes (RuO_2/MWCNT) deposited by magnetron sputtering [38]. Both, the nanostructured nature and porosity of the sensing film may improve the response time of the sensor. It is also observed that the sensor shows faster response in acidic solutions than in basic solutions, and this may be related again to ion exchange of small mobile H^+ dominant in such solutions [38]. With SEs based on RuO_2 with glass addition (mainly commercial pastes) we also noticed a slower response in basic solutions. This may be due to partial leaching of glass present as the component of the sensitive layer [23]. It is also found that the response time of a pH sensor made of RuO_2 commercial paste is higher with respect to sensors having glass-free RuO_2 formulation based SE. Higher glass content in the commercial paste leads to smaller open porosity and better compactness of the sensing layer. This reduces the diffusion rate of protons through the RuO_2-glass layer and results in an increased response time [23,139].

4.2. Interference effect/Selectivity

One of the major drawbacks of a MO_x pH sensor is interference effect of other ions on the sensing performance. Several reactions may occur due to the presence of different ions in a solution - both in the acidic and basic pH ranges and this affects measured potential of the sensor. The selectivity coefficient of an ion SE characterizes the ability to distinguish a particular ion from others. According to International Union of Pure and Applied Chemistry (IUPAC) recommendation, the selectivity coefficient, $K_{A,B}^{pot}$ is evaluated by means of the *emf* response of ion-selective electrodes in mixed solutions of primary ion, A, and interfering or less desirable ion, B (Fixed Interference Method, FIM), in separate solutions of A and B (Separate Solution Method, SSM) [140]. The interfering impact of common anions (Cl^-, Br^-, SO_4^{2-}) and cations (Li^+, Na^+, K^+, Ca^{2+}) is usually insignificant in majority of MO_x based pH sensors [23,37,82]. However, from the literature it is clear that the SEs made of commercial pastes show susceptibility to interferences caused by common anions such as halide, sulphate, carbonate ions due to the presence of lead in the SE [139]. The influence ions in sensor performance purely depends on type of materials and concentration of ions in the solution.

4.3. Drift effect

Drift effect refers to the slow non-random change of output voltage of the SE with time in a solution with constant composition and temperature. The drift rate increases while increasing the pH value of solution from acidic to basic. Bousse and Bergveld [141] suggested that presence of OH^- ion is one of the factors that causes the observed higher drift in alkaline solutions than in acidic solutions [65,141]. According to Zhuiykov [59], the RuO_2 sensing electrode shows a voltage drift during the initial month of testing. This is due to the H^+ transport through SE which is governed by H_2 trapping at the trap site existing at the grain boundaries or micro-pores of the nanostructured SE [59]. The drift in potential also depends on the experimental temperature; when temperature is high, pH-response drift is significant for the first few days and thereafter stabilized very fast. Even though the method of deposition of SE is similar, the sensors may exhibit different drift rates [65]. The drift effects of few MO_x materials are presented in the Table 1. Table 1 reveals that, several factors such as the measurement circuit, quality and composition of the SE, type of materials, thickness, surface homogeneity and porosity of the sensitive layer significantly influence the drift effect.

Table 1
Drift effect for a few MO_x based pH sensors.

Materials	Method of fabrication	Drift Effect	Ref
RuO_2	radio frequency sputtering	pH 4: 0.13 mV/pH; pH 7: 0.38 mV/pH; pH: 10 7.31 mV/pH	[58]
RuO_2	screen printing	± 1.5 mV/month (after 15 days of measurement)	[59]
IrO_2	electrodeposition	pH 1: 0.02 pH/h pH 7: 0.003 pH/h pH 11: 0.07 pH/h	[57]
IrO_2	sol–gel	3–10 mV	[40]
Ta_2O_5	radio frequency sputtering	pH 7: 0.03–0.05 mV/day	[71]
Ta_2O_5	electron-beam evaporation	pH 7: < 0.5 mV/h (after 3 h); 0.2 mV/h (after 10 h)	[142]
WO_3	radio frequency sputtering	pH 1: 1.5 mV/h pH 3: 3.6 mV/h pH 5: 6.6 mV/h pH 7: 15.7 mV/h	[143]
WO_3	magnetron sputtering	< 3 mV	[73]
TiO_2	sol–gel	pH 7: 1.97 mV/h	[61]
TiO_2	radio frequency sputtering	1.67 mV/h	[144]

Table 2
Hysteresis effect of a few MO_x based pH sensors.

Materials	Method fabrication	pH loop/values	Hysteresis (mV)	Ref
RuO_2	radio frequency sputtering	7-4-7-10-7	4.36	[58]
		7-10-7-4-7	2.2	
RuO_2	magnetron sputtering	7-4-7-10-7	6.4	[38]
		7-10-7-4-7	5.1	
		2-8-12-8-2	10.2	
IrO_2	sol-gel	1.50, 2.81, 3.75, 6.28, 7.86, 9.52 and 10.50	23.7, 9.5, 0.3, 14.5, 16.5, 6.7, and 11.5	[40]
IrO_2	Electrodeposition	2-10-2	2.5 ± 0.6	[56]
IrO_2	electrodeposited	7	1.5-0.5	[57]
WO_3	magnetron sputtering.	2-12	< 13	[73]
WO_3	radio frequency sputtering	3-1-3-5-3	7.2	[143]
		5-3-1-3	12.5	
		4-1-4-7-4	12	
		4-7-4-1-4	26	
		3-1-3-5-3	7.2, 9.7 and 15.4 (10, 20 and 40 min)	
Ta_2O_5	radio frequency sputtering	7-4-1-4-7-10-7	~5	[70]
Ta_2O_5	electron-beam evaporation	3-10	1.5-9	[142]
Ta_2O_5		6-2-6-12-6	15.2 and 0.3 (without and with post annealing)	
			6.3 and 0.7 (without and with post annealing)	
		6-12-6-2-6		
SnO_2	radio frequency sputtering	7-10-7-4-7	< 3	[145]
		7-4-7-10-7	< 7	
		7-2-7-12-6	7.3	
SnO_2	sol-gel	5-1-5-9-5	3.74	[83]
		4-1-4-7-4	1.3	

4.4. Hysteresis effect

The memory or hysteresis effect arises when a pH electrode which has been used several times in the same pH buffer solution leads to random output voltages [58,102]. The hysteresis width in acidic region of solution is smaller than in alkaline solution since the diffusion speed of H^+ ions is faster than OH^- ions. One of the interesting observations in MO_x based sensors is the dependence of hysteresis width on measurement loop time. It was found that the hysteresis width increases with increasing loop time [65]. Few reports on hysteresis and new materials and methods indicate that the hysteresis effect is lower in the case of MO_x pH sensors. For comparison, corresponding to the hysteresis widths observed in different pH sensors based on MO_X, we investigated the measured potential value for different loop values and a few of them are presented in Table 2. Hence, the hysteresis width of MO_x pH sensor strongly depends on the pH measurement loop and time of measurements, the surface area and crystalline properties of the materials.

5. Sensing mechanism

Researchers have invested considerable effort on identifying the sensing mechanism of MO_x based pH sensors. Five different mechanisms considered by Fog and Buck [52] to explain pH sensitivity of MO_x include: (i) simple ion exchange in a surface layer containing –OH groups, (ii) a redox equilibrium between two different solid phases, (iii) redox equilibrium involving only one solid phase whose hydrogen content can be varied continuously by passing current through the electrode, (iv) single phase 'oxygen intercalation' of the electrode and (v) a steady state corrosion of the electrode material. Among these, the 'oxygen intercalation' is found to provide closest explanation for mechanism for pH sensitivity [139]. Following the explanation by Fog and Buck [52], Trasatti [146], Mihell and Atkinson [147] have also suggested that the pH response could be due to ion exchange in surface layer containing −OH groups. In general, when the sensor comes into contact with a solution, the MO_x surface gets covered by hydroxide groups due to dissociative adsorption of water. The oxide sites formed by releasing protons can result in formation of a couple of higher and lower valency MO_x and lead to generation of a potential difference between the SE and RE. The magnitude of this potential is proportional to pH of the solution according to the Nernst equation [37]:

$$E = E_0 - \frac{2.303RT}{nF}pH \quad (1)$$

where E is electromotive force (*emf*) of the electrochemical cell, E_0 is standard potential, R is universal gas constant, T is absolute temperature, n is the number of electrons and F is Faraday constant. At temperature T equal to 25 °C and for one electron electrode reaction, the slope factor of the plot is 59.14 mV/pH.

As per site-binding theory [61,148,149], after immersion in an aqueous solution, formation of surface groups −O−, −OH and $-OH_2^+$ occurs for a majority of oxides, as illustrated in Fig. 6a. Protons and hydroxide ions from the solution get attracted to oxygen ions from the MO_x crystal lattice and to the surface cations, respectively. This results in the covering of MO_x by hydroxide groups. The created metal hydroxide groups can donate a proton to the solution and form a negative surface group or accept a proton from the solution converting into a positive surface group [61,70,148,150]. The charged surface groups at the MO_x- solution interface create

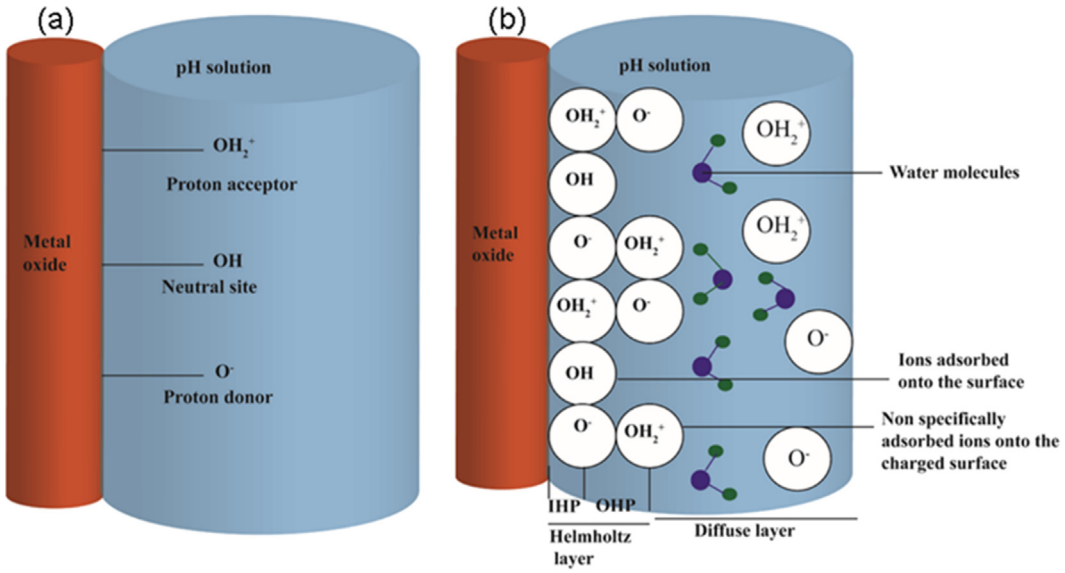

Fig. 6. (a) Schematic representation of the site-binding theory of a MO_x based pH sensor and (b) adsorption of potential determining ions on the surface and the formation of *edl* structure.

an *edl* structure, as shown in Fig. 7b. The *edl* consists of the Helmholtz layer (compact layer) and the diffuse layer (Stern layer). The Helmholtz layer contains inner Helmholtz plane (IHP) and outer Helmholtz plane (OHP), as illustrated in Fig. 6b. The charged surface groups are located in IHP and are strongly adhered to MO_x surface by chemical bonding. In OHP, the ions from the solution are attracted to the surface charge by Coulombic interaction. In the diffuse layer, ions in the solution move freely due to thermal or electrical forces [92,148,149]. These reactions may occur due to the involvement of diffusion of ions, adsorption of ions or be related to both diffusion and adsorption of ions at the MO_x surface [70,92].

A change in the pH value of a solution affects the equilibrium state of MO_x surface, which may lead to changes in electrical properties and surface potential (Ψ) of the SE [61,92,109,151,152]. The variation in electrical properties of *edl* depends on the nature of electrode material and its chemical reactivity at the solution interface. To investigate the sensing mechanism of pH ISFET, Liao et al. [61] carried out detailed experimental and theoretical study based on site binding theory at the point of zero charge pH_{PZC} and surface potential of a tin oxide gate ISFET. The changes of Ψ of MO_x can be described as [61]:

$$2.303(pH_{PZC}-pH) = \frac{q\psi}{kT} + \sinh^{-1}\left[\frac{q\psi}{kT}\frac{1}{\beta}\right] \tag{2}$$

where β reflects the sensitivity of the gate insulators and depends on the surface density of hydroxyl groups.

$$\beta = \frac{2q^2N_s(K_aK_b)^{12}}{kTC_{DL}} \tag{3}$$

Here, K_a and K_b are dissociation constants related to acidic and basic equilibrium, N_s is the total number of surface sites per unit area. The pH sensitivity is higher, and the response is more linear when N_s is larger. The value of N_s depends on the crystalline structure of material. C_{DL} is a double layer capacitance derived from the Gouy–Chapman–Stern model.

6. Overview of different metal oxides for pH sensor fabrication

6.1. Ruthenium oxide (RuO_2) based pH sensors

RuO_2 is a versatile and attractive MO_x which finds applications in electrochemical sensors, electrocatalysis and supercapacitors [52,150,153]. RuO_2 is a mixed electronic ionic conductor with the stable rutile structure. Compared to other pH sensitive metal oxides, RuO_2 based pH sensors have been found to exhibit outstanding sensing performance over wide pH ranges (2–12) due to their chemical stability and high conductivity which inhibit the space charge accumulation. Their significant advantages over the conventional glass pH electrode and other MO_x based pH electrodes include high sensitivity, fast response, long lifetime, low sensitivity to interferences caused by different ions, negligible hysteresis effect, and excellent repeatability (some of the features are mentioned in Tables 1, 2 and 3). Fog and Buck [52] suggested two main reasons for pH response in RuO_2 metal oxide – “oxygen intercalation” and ion exchange in a surface layer containing −OH groups. McMurray et al. [139] and Trasatti [146] have also confirmed this mechanism. There are many studies which have reported the use of RuO_2 alone or combined with other oxides for pH sensitive electrodes. Several methods, including thick film technology, have been employed for RuO_2 based pH sensor fabrication

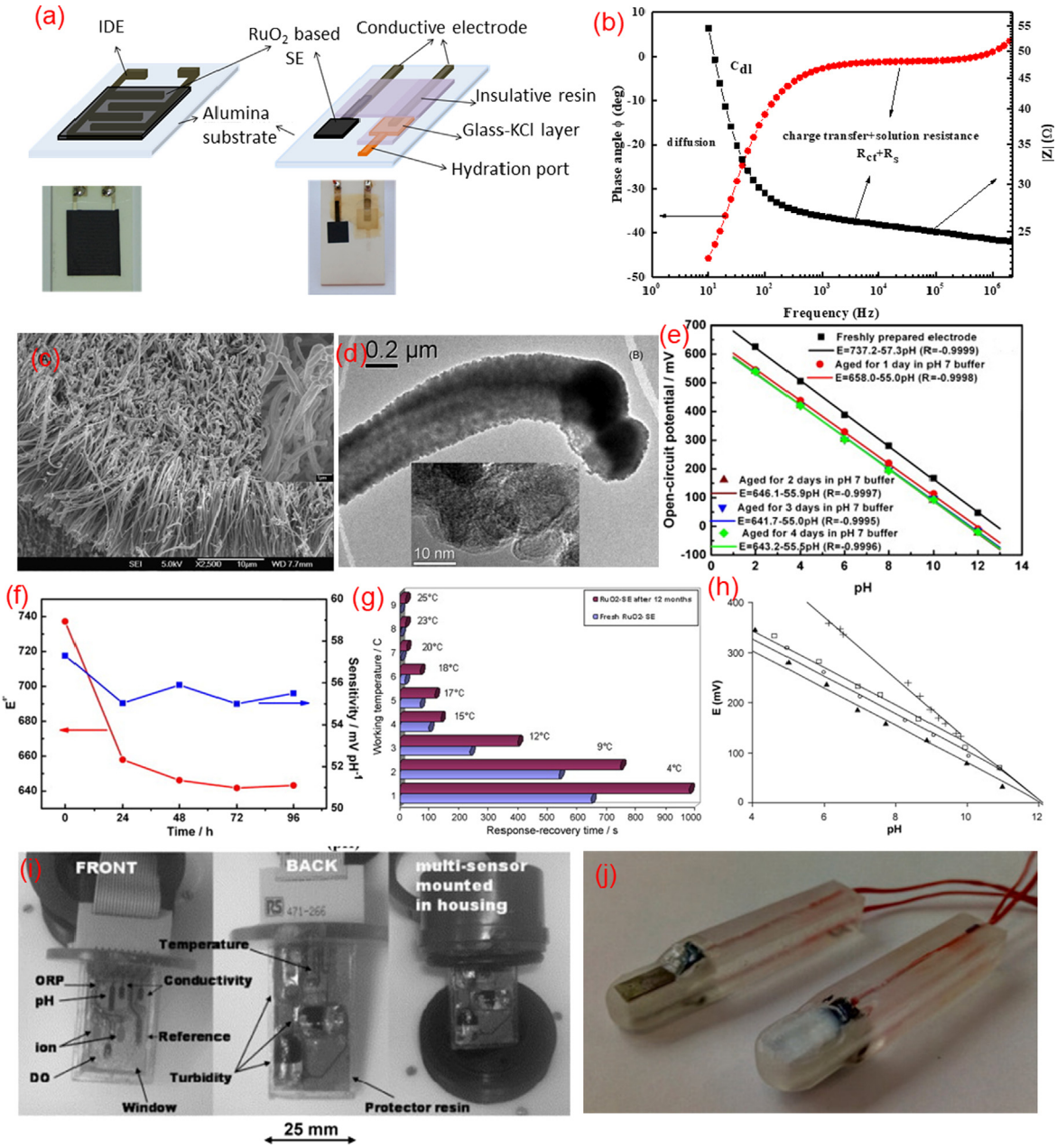

Fig. 7. Schematic view and microscopic images of the (a) RuO_2 based pH sensors (I) conductimetric, (II) potentiometric, *"Reprinted from Publication* [102] *with permission from Elsevier"*. (b) representation of impedance spectroscopic analysis explaining the diffusion, charge transfer and solution resistance of the RuO_2 based pH sensor. (c) and (d) SEM and TEM images of the RuO_2/MWCNTs nanocomposite, "*Reprinted from Publication* [38] *with permission from Elsevier"*, (e) pH response curves with different immersion time in pH 7 buffer solution, "*Reprinted from Publication* [38] *with permission from Elsevier"*, (f) the effect of time on potential and sensitivity of the RuO_2/MWCNTs electrode in buffer solutions "*Reprinted from Publication* [38] *with permission from Elsevier*". (g) response/recovery time for both freshly prepared $Bi_2Ru_2O_{7+x}$ + RuO_2-SE and after use for 12 months "*Reprinted from Publication* [159] *with permission from Elsevier"*. (h) potential vs. pH of thick film electrode of ruthenium oxide in presence of Cl- (□), Br- (○), SO_4^{2-} (▲) and NO_3^- (+) "*Reprinted from Publication* [82] *with permission from Elsevier"*. (i) multi-sensor for water quality monitoring "*Reprinted from Publication* [2] *with permission from Elsevier"*. (j) 3D printed pH sensors, RuO_2 working electrode (left) and RuO_2-PVB-SiO_2 reference electrode (right) "*Reprinted from Publication* [42] *with permission from Elsevier"*.

[20,59,60,154,155].

McMurray et al. [139] reported a pH sensor with $RuO_2{\cdot}xH_2O$-lead borosilicate glass composite as a sensing material. The sensor with RuO_2: glass ratio of 1:1 shows near-Nernstian potential in the pH range 2–12 with response time about 90 s and maximal hysteresis of 30 mV. It was noted that higher glass content in the SE causes smaller open porosity. This leads to decrease in the

Table 3
Methods of fabrication and properties of MO_x based electrochemical pH sensors.

Materials	Fabrication method	pH range	Sensitivity (mV/pH)	Response Time	Ref.
RuO_2	RF sputtering	1–13	55.64	–	[58]
Pt-doped RuO_2	Screen printing	2–13	58	1–2 s	[59]
RuO_2-TiO_2	Pechini method	2–12	56.03	–	[84]
RuO_2-TiO_2	Screen printing	2–12	56.11	< 15 s	[60]
$Bi_2Ru_2O_{7+x}$-RuO_2	Screen printing	2–13	58	–	[159]
RuO_2-commercial paste	Screen printing	4–11	57	–	[82]
RuO_2-commercial paste	Screen printing	1–12	57 ± 3	< 5 s	[22]
RuO_2-commercial pastes	Screen printing	2–11	60.01 and 60.78 – in RuO_2 1 and 10kΩ/sq.	–	[94,155,227]
Ni-RuO_2	Thermal decomposition	1.5–12.5	52 ± 2	–	[228]
RuO_2·xH_2O: Glass mixture	Hand painting	2–12	59	–	[139]
RuO_2·xH_2O mixed with polymer paste in 1:2 wt ratio.	Screen printing	2–10	52.1	–	[147]
Graphite based ink with 9.8% RuO_2(disposable pH sensor)	Screen printing	2–9	51	–	[160]
RuO_2 nanoparticles-MWCNT	Magnetron sputtering	2–12	55	< 40 s	[38]
RuO_2-Ta_2O_5	Screen printing	2–12	56	< 8 s and < 15 s in acidic and basic solution.	[23]
RuO_2-SnO_2	Screen printing	2–12	56.5 ± 0.7	< 5 s and 9 s, for acidic to basic and basic to acidic solution changes	[102]
IrO_2 (flexible sensor)	Dip coating	1.5–12	51.1	0.9 s for pH 3.9–11 2 s for pH 12–3.5	[40]
IrO_2	Carbonate melt oxidation	1–13	58.4 ± 0.2	–	[55]
IrO_2-TiO_2 (30–70) mol%	Pechini method	1–13	59.1 ± 1.47	120 s - pH 4–12 10 s - acidic region 5 s- basic region	[85]
IrO_2	Electrodeposition	3–11	72.9 ± 0.9	–	[57]
IrO_2	Anodic electrodeposition	2–10	63.5 ± 2.2	0.5, 1.5, and 1 min for pH regions < 5, 5–7, and > 7	[56]
Ta_2O_5	Sputtering	2–12	58–59	< 0.3 s	[71]
Ta_2O_5-EIS	Electron beam evaporation	2–12	57 ± 1.5	–	[142]
Ta_2O_5	Screen printing	2–10	45	–	[69]
Ta_2O_5-EIOS	Sputtering and thermal oxidation	1–10	56.19 ± 2 After 1 year 49.59 ± 2	–	[70]
SnO_2/Al	Sputtering	2–10	58	–	[67]
SnO_2-EGFET	Hydrothermal method	1–13	55.18	–	[181]
SnO_2	RF sputtering	2–12	58.1	–	[65]
SnO_2/ITO	RF sputtering	2–12	59.9 ± 1.037	–	[66]
TiO_2	MOCVD	1–13	57.4–62.3	–	[62]
TiO_2	Spin coating	1–11	58.73	–	[61]
TiO_2 nanotube array modified Ti electrode	Anodization of Ti substrate electrode	2–12	54.6 After irradiation with UV rays − 59.3	< 30 s	[63]
TiO_2 and Ru doped TiO_2 (TiO_2 :Ru)	Co-sputtering EGFET	1–13	37.73 -TiO_2 - 55.20 - TiO_2:Ru	–	[144]
WO_3/MWNT	Magnetron sputtering	2–12	41	< 90 s	[73]
WO_3	RF sputtering	1–7	44.85, 47.90, 50.10, 52.85 and 55.80 at 25, 35, 45, 55, and 65 °C respectively	–	[143]
W/WO_3	Electro oxidation	2–12	53.5 ± 0.5	For pH 6–7- 3 s, For high pH-15 s	[74]
Amorphous WO_3	RF sputtering	1–7	50	–	
CeO_2 $Ce_{0.8}Sm_{0.2}O_2$ $Ce_{0.8}Zr_{0.2}O_2$	Screen printing	7.2–10.8	38 ± 4 -CeO_2 40 ± 4 -$Ce_{0.8}Sm_{0.2}O_2$ 51 ± 2 -$Ce_{0.8}Zr_{0.2}O_2$	–	[212]
PbO_2	Transformation into α-PbO_2 and β-PbO_2 by oxidation in alkaline and acidic solutions	1–12	57.96 –α-PbO_2 57.80 -β-PbO_2	–	[213]
PbO_2	Electrodeposition	1.5–12.5	64.82 - α-PbO_2 57.85 - β-PbO_2	1 s and < 30 s in acidic medium and in alkaline solutions	[214]
PbO_2 based graphite epoxy	PbO_2-graphite epoxy composite was inserted into the glass tube.	1–11	58.7 ± 0.3 and 60.8 ± 0.2 in aqueous and aqueous ethanolic solutions	< 15 s	[229]

(*continued on next page*)

Table 3 (*continued*)

Materials	Fabrication method	pH range	Sensitivity (mV/pH)	Response Time	Ref.
MnO_2	Solid state reaction	2–12	78.3	Few seconds in acidic and basic solutions	[218]
Cobalt oxide	Screen printing	1–12	54.9–60.3	< 1 min	[220]
MnO_2/GPLE	Electrodeposition	1.5–12.5	57.051	20 s in acidic medium and 60 s in alkaline medium	[226]

diffusion rate of protons through the porous RuO_2-glass composite, resulting in decreasing response time of the metal oxide electrode. They observed that, the interference by Ca^{2+}, SO_4^{2-} ions was found to be minimal, although Cl^- ions cause a potential deviation of 20 mV [139]. The response to pH changes of the sensors can be affected by storage environment of SE. Mihell and Atkinson [147] investigated the sensors kept for longer duration in different solutions: diluted HCl, diluted KOH, deionized water and solution with pH = 6, and found a strong influence of storage conditions on the sensing performance. Zhuiykov [59] recommended storing in deionized water before measurement to enhance the stability and sensing performance of the RuO_2 based pH sensor.

Doping of RuO_2 or mixing with other oxides improves the sensing performance of RuO_2 based pH sensors. The pH sensor with nanostructured Pt-doped RuO_2 electrode exhibits an excellent Nernstian response with a very fast response [59]. The use of binary MO_x has been considered as one of the most effective methods for improving the electrocatalytic properties, sensing performance and stability of pH sensors [23,60,84,93,102]. The binary MO_x are often utilized as dimensionally stable anodes (DSA) for various applications including chloro-alkali industry, water electrolysis, oxidation of organics, organic synthesis, etc. [156–158]. In the binary MO_x system, an active transition oxide (RuO_2, IrO_2, etc.) is mixed with a chemically inert oxide, like Ta_2O_5, SnO_2, TiO_2, etc. The addition of inert oxides decreases the cost and can improve the stability, electrochemical properties and service life of the electrodes [156–158]. Pocrifka et al. [84] developed RuO_2-TiO_2 based pH SE by Pechini method (thermal decomposition of a polymeric precursor containing metallic cations) which showed a sensitivity of 56.03 mV/pH and good stability [84]. The Pechini method allows the sensor fabrication at low temperature and it has future potential advantages in flexible RuO_2 based pH sensor fabrication.

We have reported the development of new thick film SEs based on binary MO_x, such as RuO_2-TiO_2 [60], RuO_2-Ta_2O_5 [23,93,101] and RuO_2-SnO_2 [102] for potentiometric and conductimetric pH sensors, as shown in Fig. 7a. X-ray photoelectron spectroscopy (XPS) studies carried out for RuO_2-TiO_2 and RuO_2-Ta_2O_5 layers confirmed the dependence of the surface elemental composition on the pH value of a solution used for sensor treatment [60,93]. The degree of surface hydroxylation was proved to be correlated with pH change. Larger scale adsorption of hydroxyl groups and water at the surface was observed for the samples conditioned at pH of 4 and 10 as compared to those freshly prepared or conditioned in neutral water (pH = 7). The highest surface hydroxylation was found to occur for the alkaline solution (pH = 10). It was revealed that Ru ions in the sensing layer have different oxidation states (+4 and + 6). Stabilization or creation of mixed oxide phases was observed at pH of 4 and 10 while neutral environment probably led to the dissolution of these phases [60]. The potentiometric measurements showed that thick film pH sensors with the RuO_2-rich sensing electrodes obey Nernstian behavior with sensitivity close to the theoretical value for the one electron electrode reaction. Thick film pH sensors based on RuO_2-TiO_2 [60], RuO_2-Ta_2O_5 [23] and RuO_2-SnO_2 [102] exhibit a very fast response, long lifetime, reproducibility, resistance to interferences caused by ions such as Li^+, Na^+ and K^+ as well as low hysteresis and drift effect. The EIS analysis reveals that the capacitance, conductance, absolute value of impedance and phase angle of the conductimetric sensors in the low frequency range are strongly dependent on the pH value of a solution. The complex plane impedance spectra of the thick film IDE pH sensors based on RuO_2 [92], RuO_2-TiO_2 [60], RuO_2-Ta_2O_5 [93], and RuO_2-SnO_2 [102] indicate that the mixed electronic and ionic conduction underlies the sensing mechanism, as shown in Fig. 7b. This mechanism is more prominent for the sensors with sensing electrodes based on RuO_2 and binary oxide compositions with higher fraction (70 wt%) of RuO_2 [93,102]. The electrochemical sensing performances of pH sensors based on several binary MO_x fabricated by different methods are compared in Table 3.

Xu and Zhang [38] developed a RuO_2/MWCNTs nanocomposites based sensor to monitor pH. RuO_2 was deposited on vertically aligned MWCNT by magnetron sputtering. The morphology of the obtained composite is shown in Fig. 7c and d which depict the uniform distribution of the tubular MWCNT (in SEM image) and a magnified view of the tubular cross section near the edge of a single tubular structure due to coating of RuO_2 (in TEM image), respectively. The freshly prepared sensor shows a sensitivity of 57 mV/pH as presented in Fig. 7e. However, after immersing the sensor in pH 7 buffer solution for 24 h the sensitivity is reduced to 55 mV/pH. The effect of immersing time on sensitivity and E_0 is shown in Fig. 7f. After 24 h of immersion in pH 7 buffer solution, the E_0 and sensitivity value were almost stable [38]. The observed initial drift in potential and sensitivity is due to the hydration reactions at the RuO_2 electrode surface and similar behavior was also reported by Zhuiykov [59] as well as in our previous work [60] on RuO_2 based pH sensors. Zhuiykov [159] developed a new sensing material based on $Bi_2Ru_2O_{7+x}$-RuO_2 for online monitoring of pH of water. Due to the lead content in the commercial RuO_2 paste, pH sensing electrode often shows poor selectivity in the presence of halide, sulphate and carbonate ions in water. Application of this new material enabled the author to reduce the lead content and restrict its detrimental impact on the measurement results. It was also observed that in warm water, the sensor's response to pH changes was much faster than in cold water (shown in Fig. 7g). The measurement (Fig. 7g) shows the response/recovery rates for the freshly prepared and the sensor used for 12 months. When the sensor was stored in water, the sensor response/ recovery rate is influenced by the biofouling effect. In the subsequent study, Zhuiykov et al. [39] investigated the influence of the thickness of Cu_2O doped RuO_2 electrode on the sensing performance of pH sensor which we have already discussed in Section 4.1.

It was found that ions: Cl^-, NO_3^-, SO_4^{2-}, F^-, I^-, Ca^{2+}, K^+ have little influence on the sensing performance [2,22,82]. However, RuO_2 sensitive electrode made of a commercial paste shows susceptibility to interferences caused by anions and slow response in basic solution. Labrador et al. [82] developed a theoretical model to determine the response of thick film pH sensor based on the commercial RuO_2 paste. The experimental analysis of the interferences of common anions obtained by the fixed interference method is presented in Fig. 7h. The model explains the redox potential behavior of complex electrodes containing a mixture of MO_x involved in redox processes and enables evaluation of interfering influence of some anions. The sensing performance and methods of fabrication of a few RuO_2 based sensors are also listed in Table 3.

One of the major reported applications of RuO_2 based pH sensors has been water quality monitoring. Martinez-Manez et al. [22] developed a multi-sensor by thick film technology (screen printing) for monitoring water quality parameters in making use of the RuO_2 sensing layer for determining the pH of water. Other water quality parameters such as DO (dissolved oxygen), temperature, turbidity and conductivity were also determined. This multi-sensor applied for online monitoring of water pollution seems to solve the drawbacks of traditional systems employed for this purpose [22]. For online monitoring of water pollution, Zhuiykov [2] and Atkinson et al. [20] developed integrated multi-sensors with pH sensors based on RuO_2 sensing electrodes (shown in Fig. 7i). Furthermore, RuO_2 based pH sensor was also utilized for measuring pH of several beverages. Koncki and Mascini [160] demonstrated a disposable pH sensor prepared by screen printing technique and studied its potential application for pH analyzing of food drinks, like Fanta, wine, milk, cola and orange juice. The obtained results were comparable with those determined using a conventional glass pH electrode. We had developed a new LTCC based pH sensor aimed at miniaturization, cost reduction and integration of the sensor part with passive components in a single substrate for wireless application [23,101]. These potentiometric pH sensors with the SEs based on commercial RuO_2 paste as well as the prepared RuO_2-Ta_2O_5 and RuO_2-Ta_2O_5-glass compositions fabricated by LTCC technology exhibited excellent sensing performance. The developed LTCC based pH sensors were also successfully tested in wireless monitoring system [23,101]. Liao and Chou [58] used RuO_2 thin film as a hydrogen sensing layer in an ISFET type sensor. This pH sensor was also applied for measuring pH of a few fluid foods, like cola, yogurt, water and milk [10,42,154]. For this application, RuO_2 sensitive electrode printed on alumina substrate and a pseudo reference electrode (RE consisting of a thin film of RuO_2 electrode modified with a polyvinylbutyral (PVB)-SiO_2 layer) embedded in 3D printed housing (shown in Fig. 7j) were used [42]. The measured pH values are in good agreement with those obtained using the conventional glass pH electrode. The fabricated 3D printed device exhibited its potential application for the online water quality monitoring and glass free pH sensor applications.

6.2. Iridium oxide (IrO_2) based pH sensor

Among different MO_x for pH sensors, IrO_2 has shown excellent stability over a wide pH range at high temperature up to 250 °C, at high pressure, and in aggressive environment, as well as a fast response even in non-aqueous solutions [161,162]. IrO_2 crystallizes in the rutile structure [163] similar to RuO_2 but exhibits lower catalytic activity than RuO_2. Besides its pH sensing application, IrO_x is also well known as an anode material for oxygen and chlorine evolution and as an electrochromic material [164,165]. The characteristics of IrO_x sensors are very sensitive to the film structure and composition, which depend on the fabrication procedure (a few works are mentioned in Table 3). Considering these aspects, Katsube et al. [161] explored a pH sensor based on metal-MO_x configuration, an IrO_2 film deposited by sputtering method on various substrates including titanium and tantalum. The sensing electrode was stable in aqueous solutions at temperatures up to 200 °C. The films sputtered on stainless steel and tantalum substrates show a Nernstian response with the slope factor of 59 mV/pH. It was found that due to different structure of the film the electrochemical reactions occurring at the IrO_2 film prepared by sputtering and anodization methods are different.

The sol-gel method can provide a simpler and economically feasible approach for low temperature fabrication of iridium oxide film. Nishio et al. [166] adapted dip coating process for preparation of IrO_2 film. For the fabrication of SE, iridium chloride was used as a starting material in solution preparation and the deposited film was heat treated at 300 °C. Based on Nishio et al. [166] work, Huang et al. [40] developed a flexible IrO_2 pH sensor on a polymeric substrate as shwon in Fig. 8a. The sensor shows a sensitivity of 51.1 mV/pH in the pH range of 1.5–12 at 25 °C [40]. This flexible sensor exhibits excellent sensitivity, response time, stability, reversibility, repeatability and selectivity [40]. Based on this work, Nguyen et al. [167] fabricated pH sensors array, consisting of 16 individual sensors (SE based on IrO_2 and RE based on Ag/AgCl) on a single polyamide flexible substrate by sol-gel method. For mapping pH value across the surface, a thick layer of PDMS polymer with 4 × 4 punched-out wells (with a diameter of 5 mm) was placed on top of the surface of the sensors and all the sensors were conformed on the outer surface of a plastic tube (3.5 cm in radius) for measurement. This experimental setup ensured that the test solutions stayed on the top of individual sensors without mixing with each other. The developed sensors in arrays exhibit sensitivity close to Nernstian responses in the range of 57.0–63.4 mV/pH [167].

The Ir salts are more expensive than Ru salts, for reducing the cost of IrO_2 SE, Da Silva et al. [85] prepared a binary oxide IrO_2-TiO_2 and utilized polymeric precursor method for the sensor fabrication. They developed SE on titanium substrate based on the composition of IrO_2-TiO_2 with (100–0), (70–30), (30–70) and (20–80) mol%. The electrode based on IrO_2-TiO_2 (30–70) mol% in the range of pH 1–13 shows excellent sensitivity, fast response and good reproducibility [85]. Wang et al. [55] have reported a new method based on chemical oxidation called 'carbonate melt oxidation' for developing iridium pH electrode with long-term stability. Iridium metal wire was coated with a uniform iridium oxide film by oxidation of the wire in a carbonate melt. In a wide pH range, this pH sensor exhibits excellent sensitivity and long lifetime. Moreover, it is suited for continuous pH measurement without the need of frequent calibration [55]. IrO_2 based micro-electrochemical transistor for pH sensing fabricated by anodic electrodeposition was reported by Pasztor et al. [168]. The sensor shows the sensitivity of 65 mV/pH, higher than the theoretical value in the pH range 1.8–12, and the response time of 40 s. A pH sensor fabricated by anodic electrodeposition of IrO_2 film was also developed by Marzouk et al. [56] for physiological application such as measurement of extracellular myocardial acidosis during acute ischemia. Such

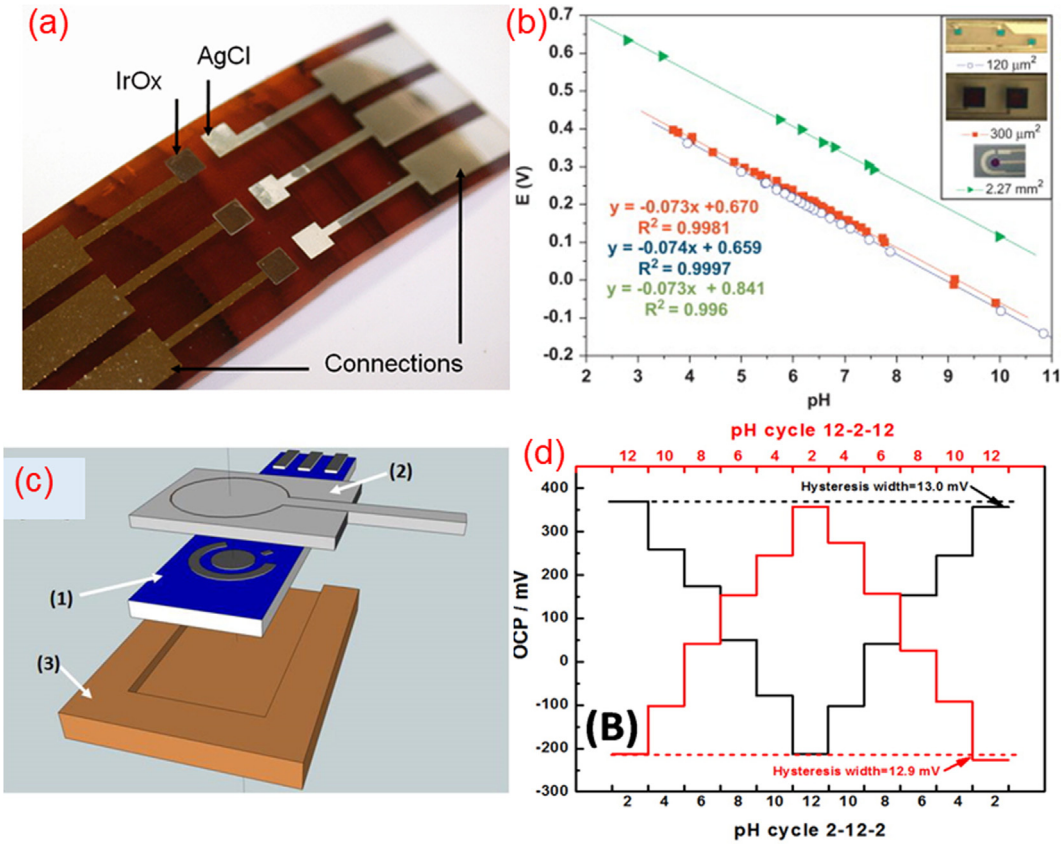

Fig. 8. Image of three pairs of flexible IrO_2 seneing electrode and AgCl reference electrode "*Reprinted from Publication* [40] *with permission from Elsevier*". (b) potentiometric response of three pH sensing electrode with increasing area (120, 300 μm^2 and 2.27 mm^2) and inset show the sensor "*Reprinted from Publication* [57] *with permission from Elsevier*". (c) Schematic diagram for electrochemical paper-fluidic pH sensor (1) IrO_2-rGO-SE, (2) μPAD with hydrophobic pattern and (3) ABS holder "*Reprinted (adapted) with permission from* [138] *Copyright (2016) American Chemical Society*. (d) Hysteresis width of IrO_2-rGO at pH 2–12–2 and 12–2–12 loop cycles"*Reprinted (adapted) with permission from* [138] *Copyright (2016) American Chemical Society*.

method has potential applications in developing pH sensors on flexible substrates for wearable applications.

Kinlen et al. [169] developed a new approach for fabrication of pH sensor which is based on a polymer Nafion-coated IrO_2 electrode and a polymer modified Ag/AgCl RE. The Nafion layer on IrO_2 surface after annealing becomes permselective to cations. Maintaining the electrode sensitivity to pH, it eliminates or attenuates many of anionic interferences. The authors reported that the polymer based RE is helpful to trap the Cl^- ion in the polymer layer by encapsulating it with a Nafion outer layer. After annealing, the Nafion membrane effectively blocks Cl^- diffusion to the test solution and maintains a constant Cl^- activity on the AgCl surface, and thus a constant electrode potential. Hence, by applying this method one of the drawbacks of a MO_x pH sensor, related to response to redox species in the solution which leads to errors in pH measurement, can be avoided [169].

IrO_2 based sensors received promising applications in many fields including biomedical ones. Kreider [162] fabricated by sputtering IrO_2 pH sensor suitable for high temperature, high pressure application in the nuclear repositories system. The sensor shows a linear response of approximately 53–58 mV/pH at room temperature in a wide range of solution conditions. For a biomedical application, Prats-Alfonso et al. [57] reported a urea biosensor based on anodic electrodeposited iridium oxide film pH electrodes modified with urease coated magnetic particles. They observed the area of the electrode does not have significant differences in sensitivity (slope shown in Fig. 8b). For environmental application, recently Yang et al. [138] proposed fully portable pH sensor based on IrO_2-rGO sensitive layer. The device consists of an integrated miniaturized programmed paper-fluidic electrochemical pH platform (schematic representation is shown in Fig. 8c) integrated with portable pH meter powered by batteries to make digital pH test strips for in-field measurements. The major advantage of pH platform is that it combines advantages of both pH strips and pH meters for water quality monitoring. The IrO_2 – rGO SE exhibited a slightly super Nernstian response (61.7 mV/pH) in the range of pH 2–12 with response time less than 250 s and hysteresis width 13 mV in different cycle shown in Fig. 8d [138].

Monitoring the stability of pH of organs such as the heart is an important biomarker in health monitoring. However, the traditional electrochemical pH sensor using glass electrode is not able to be utilized in such application because it is rigid, hard, shows bulky behavior and provides only single measurement channel. The advanced flexible pH sensor overcomes some of these drawbacks of the glass electrode. However, the limitation of stretchability or possibility to conform to complex three-dimensional surfaces of

flexible sensor prevent applications areas of the heart in ways that do not constrain natural motions. Chung et al. [170] developed IrO_2 based stretchable arrays of pH sensors. It was found that in the developed solution interconnected arrays of IrO_x pH sensors encapsulated in thin, low-modulus elastomers can yield conformal monitoring system capable of noninvasive measurements on conformal lamination onto the time-dynamic epicardial surfaces of the beating heart. The sensor shows a super-Nernstian sensitivity with excellent repeatability (69.9 ± 2.2 mV/pH). $[K^+]$ and $[Mg^{2+}]$ are the two cations that are present in the extracellular space during ischemia. It was observed that the range of potential variation with influence of these ions was less than 3.5 mV, which corresponds to ≈0.05 pH [170]. The influence of measuring media temperature is a very important factor in pH sensing mechanism. In this study the developed sensor shows a linear dependence of −1.63 ± 0.02 mV/°C for temperatures between 20 and 60 °C [170]. In addition to this for wearable application, to attach a conformal surface on the body, highly flexible sensors are required, especially for sweat monitoring applications. For this, the sensor cloth will be a great advantage and has recently been achieved by the electrodeposition of IrO_2 film on conductive cloth [171]. The developed textlie on cloth which shows sensitivity of 47.54 mV/pH for sweat monitoring. Authors observed that the sweat pH measurement in human skin using the fabricated sensor shows a relative error of 4% when compared with a standard pH measuring method.

6.3. Tantalum oxide (Ta_2O_5) based pH sensors

The materials based on Pt-group metals are very expensive, so the research interest has been directed towards the development of pH sensors using cheaper materials. Among these materials, Ta_2O_5 has received significant attention, in particular for the fabrication of pH-ISFETs due to its high sensitivity (59 mV/pH), low drift and lower surface deterioration due to oxidation [71,172]. Ta_2O_5 has found interesting applications as a proton conductor, catalyst, high dielectric constant gate insulator, optical coating material with high refractive index and low loss. For Ta_2O_5 pH-ISFET, diffusion and phenomena described by the site-binding model are known to be responsible for the sensing mechanism [71]. The crystalline structure of Ta_2O_5 film exhibits a significant influence on the sensing performance. So, heat treatment procedure of the sensing membrane has a substantial role in the sensitive layer fabrication [71]. The sensitivity of Ta_2O_5 oxide film depends on the amount of surface sites, so Ta/O ratio at the surface represents a critical parameter for the pH sensing mechanism. According to Kwon et al. [71], the Ta/O ratio in the sensing membrane is the most important parameter for the pH sensitivity. They suggested that with increasing O-sites at the surface, the sensitivity of the sensing membrane increases. A Ta_2O_5 film for pH ISFET sintered at 400 °C in O_2-ambient shows excellent pH sensitivity (58–59 mV/pH) for a wide pH range (2–12) [71].

Recently, Chen et al. [70] developed Ta_2O_5 based electrolyte-ion sensitive membrane-oxide–semiconductor (EIOS) pH sensor for online pH monitoring in an acidic environment, as shown in Fig. 10a. When Ta_2O_5 is exposed to a solution, surface hydrolysis of Ta_2O_5 takes place leading to formation of tantalum hydroxyl groups (Ta-OH). This surface becomes charged either by donating or accepting protons during reaction with solutions containing H^+/OH^- ions [70], as shown in Fig. 9a. The membrane and electrolyte interface lead to a network consisting of the double layer capacitance (C_{dl}), charge transfer resistance (R_{ct}) and Warburg impedance (W), which is associated with the diffusion of ions from the electrolyte to the membrane. In this study, a two-electrode configuration (SE – Ta_2O_5 and RE- conventional Ag/AgCl) was used for EIS analysis of the sensor. The results of EIS studies of the sensor were as shown in Fig. 9b with equivalent circuit analysis (Fig. 9c). In the lower frequency range, the sensor shows Warburg impedance due to diffusion of ions from electrolyte to the membrane, as illustrated in Fig. 9b [70]. In our previous work we observed that the electrical properties of a thick film conductimetric pH sensor based on Ta_2O_5 sensing layer are strongly dependent on the pH value in the low-frequency range. However, thick film potentiometric pH sensor with Ta_2O_5 sensing electrode exhibits a sub-Nernstian behavior. A combination of ionic exchange and electronic transfer may be the reason behind the pH sensing mechanism of Ta_2O_5 based pH sensor [69].

The breakable glass pH electrode has limitations in using for food processing applications. There is a great demand for “non-glass” pH sensors in food industry, biotechnology, water purification, etc., especially for online monitoring purpose. Schoning et al. [142] reported a pH sensor with the sensitive capacitive EIS structure (electrolyte-insulator-semiconductor) with Ta_2O_5 gate for in-line pH monitoring systems in food industry. The proposed sensor exhibits a sensitivity of 57 ± 1.5 mV/pH in the range of pH 2–12 [142]. The pH EIS based sensors with corrosion resistance against strong alkali solutions were developed by using Al_2O_3-Ta_2O_5 and Al_2O_3-ZrO_2 sensitive materials. The sensor based on Al_2O_3-Ta_2O_5 showed higher pH sensitivity while Al_2O_3-ZrO_2 layer was more effective in enhancing corrosion resistance against strong alkali solutions [173].

6.4. Tin oxide based pH sensors

Tin oxide is one of the most intensively studied semiconductor oxides for gas sensors [174,175], and little attention has been paid to its pH sensing application. Fog and Buck [52] reported that SnO_2 based potentiometric pH sensor shows a sensitivity of 48.6 mV/pH. These authors mentioned that SnO_2 in the doped form are not suitable for pH electrode fabrication, but functions mainly as a redox electrode. However, after this work only few studies were devoted to SnO_2 as a pH sensitive material due to its applicability in a narrower dynamic range as compared with glass and other metal oxide based pH sensors [176]. The major studies concerning SnO_2 pH sensors were carried out for ISFETs. Liao et al. reported SnO_2 as a pH sensitive material prepared by using thermal evaporation or sputtering method for ISFET applications and also investigated sensing mechanism of pH ISFET [177]. They concluded that surface parameter ΔpK (pK_b-pK_a) is one of the dominant factors for pH response of ISFET [125,177]. Liao et al. [177] reported that SnO_2 is a suitable pH sensitive layer regardless of deposition method. To confirm this claim, they developed different SnO_2 based pH ISFETs, such as SnO_2/SiO_2 gate ISFET (SnO_2 prepared by thermal evaporation method) which shows a sensitivity of 58 mV/pH, SnO_2/Si_3N_4/

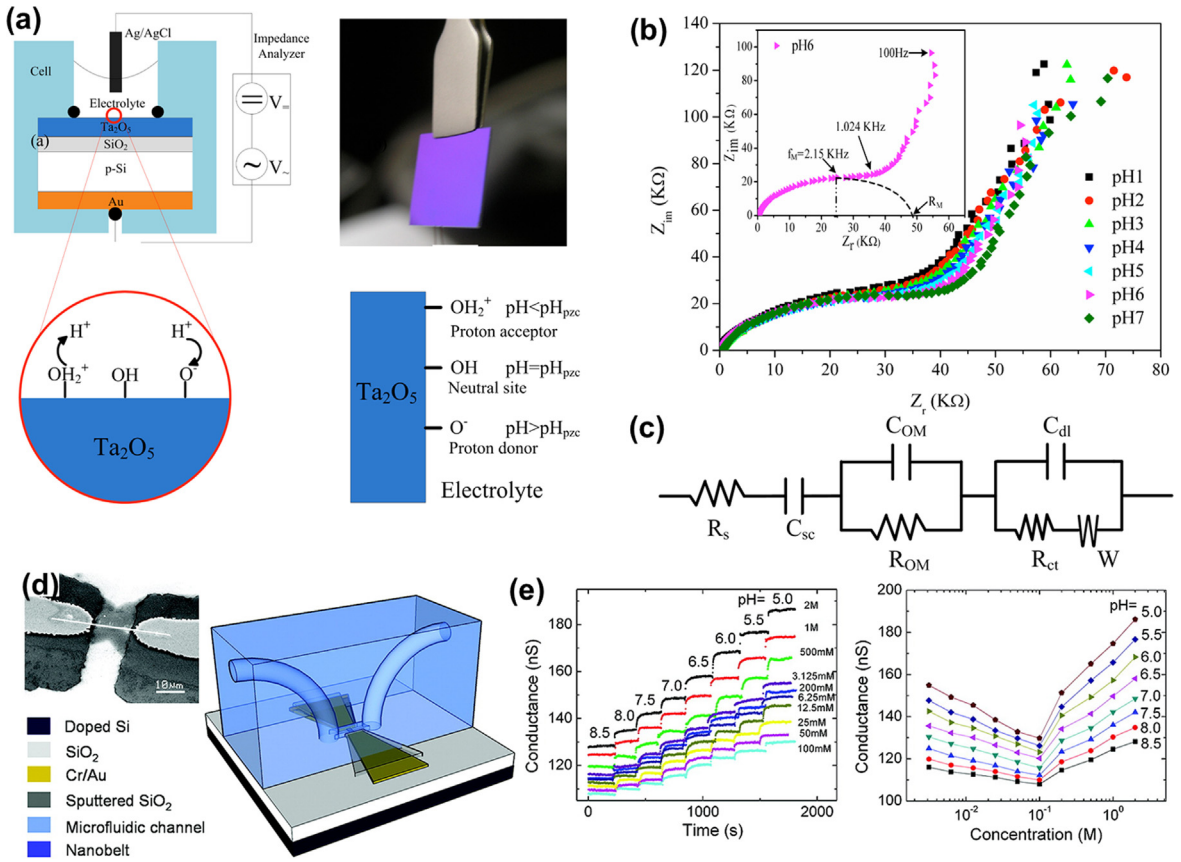

Fig. 9. (a) Scheme of the measuring setup; lab-made sensor; pH sensing mechanism at the Ta_2O_5–electrolyte interface (c) and (d) depending on the electrolyte pH, the surface groups can be neutral (OH) or negative (O^-) or positive (OH_2^+); V=: direct current bias voltage; V∼: alternating current voltage; pHpzc: pH value at the point of zero charge. For operation, a direct current polarization voltage is applied via the Ag/AgCl reference electrode to set the working point of the sensor, and a small alternating current/voltage is applied to the system to do the measurement "*Reprinted from Publication* [70] *with permission from Elsevier*".. (b) EIS spectra of Ta_2O_5 based EIOS pH sensor "*Reprinted from Publication* [70] *with permission from Elsevier*". (c) Equivalent circuit of the EIS analysis "*Reprinted from Publication* [70] *with permission from Elsevier*". (d) The 3D schematic view of a SnO_2 nanobelt FET integrated with microfluidic channel and the SEM image of a device with a SnO_2 nanobelt connecting the source/drain electrodes covered with sputtered SiO_2 *"Reprinted (adapted) with permission from* [180] *copyright (2008) American Chemical Society."* (e) real-time pH response of the device to different sodium phosphate solutions and the channel conductance as a function of ten different ionic concentrations at different pH value *"Reprinted (adapted) with permission from* [180] *copyright (2008) American Chemical Society."*

SiO_2 gate ISFET (SnO_2 deposited by r.f. reactive sputtering) with a sensitivity of 57 mV/pH) and SnO_2/SiO_2 gate ISFET (SnO_2 developed by r.f. reactive sputtering) which exhibits a sensitivity of 55 mV/pH [177].

For the open gate FET based sensors such as the conventional ISFET, the influence of light can cause a considerable voltage shift. Chin et al., [67] found that SnO_2/Al discrete gate ISFET structure prepared by the standard CMOS IC processes exhibits a sufficient decrease in light sensitivity. The SnO_2/Al discrete structure of ISFET sensor consists of an open contact window and a MOSFET transistor. The window was covered by Al and plated with SnO_2 membrane for pH sensor [67]. Since thermal behavior has a strong influence on the properties of an ISFET sensor, it is necessary to determine effective methods to improve sensor stability. To realize this purpose, Chin et al. [178] fabricated a combined pH ISFET with SnO_2/Al multilayer electrodes and p-n diode temperature sensor. These authors presented detailed theoretical considerations and experimental behavior of both sensors. The fabricated pH sensor showed a sensitivity of 58 mV/pH in the pH range of 2–10 [67].

The method of preparation of the pH electrode influences the sensing performance. For example, Fog and Buck [52] observed that SnO_2 based sensor shows a sub-Nernstian response. However, Pan et al. [176] developed a SnO_2 pH electrode on ITO substrate by sputtering method which shows sensitivity close to the theoretical Nernstian response. These authors found that for sputtering method the sensing electrode area, O_2 gas concentration and deposition pressure are influencing the pH sensing characteristics. The sensor with a SE of 4 mm^2, at 20% O_2 gas concentration and deposition pressure of 20 mtorr exhibits sensitivity of 59.17 mV/pH [176]. In a further work, Pan et al. [179] reported SnO_2 thin film membrane for real time pH sensing system of the sensor array which reduces signal errors and sensing time.

Hysteresis and drift are two phenomena which limit the accuracy of the pH ISFET sensors. There are few reports which proposed an improvement of the sensing characteristics by the control of these effects by sputtering and rapid thermal processing techniques.

Tsai et al. [145] prepared SnO_2 thick film based pH ISFET by sputtering method. They investigated sensing behavior for the pH range 2–12 and found the pH sensitivity close to the theoretical Nernstian response and very low hysteresis effect. The recent studies of SnO_2 based pH sensors have been concentrated on fabrication of EGFETs. In ISFET and EGFET structures either sapphire wafer or Si structure have been used as substrates. For reducing the cost and improving the sensing performance, Yin et al. fabricated by RF sputtering a pH sensor based on ion sensitive SnO_2/ITO glass EGFET structure [133]. For the study of sensing performance, the authors used different sensing gate structures, such as SnO_2/Al/micro slide glass, SnO_2/Al/Corning glass, ITO glass, SnO_2/ITO glass and ITO/micro slide glass. They observed that SnO_2/ITO glass based sensing gate structure of EGFET has smaller drift and hysteresis effect and good sensitivity of 57 mV/pH [133]. Li et al. [68] demonstrated for the first time an EGFET with low-temperature hydrothermally synthesized SnO_2 nanorods as the pH sensor. Batista et al. [181] reported the fabrication of a SnO_2 based EGFET pH sensor by a low-cost sol-gel Pechini method.

The majority of SnO_2 based pH sensors are fabricated using thin film technology. Only a few studies were devoted to thick film tin oxide-based pH sensors. Arshak et al. [111] investigated tin oxide sensing layers in a conductimetric IDE pH sensor. They found that both SnO and SnO_2 operated well at low frequencies giving the best response to pH change in the range of 2–11. In their work, they noted that the device with both SnO and SnO_2 electrodes cannot be utilized in reusable pH sensors [111]. Basing on EIS analysis of an IDE conductimetric pH sensor with thick film SnO_2 electrode, we suggested that the sensing mechanism of the sensor can be attributed to the occurrence of charge transfer in the high frequency range and ionic conduction in the low frequency range [102].

There is growing interest of pH sensors in biomedical applications, especially for monitoring of bio substances, such as virus, protein and DNA. A FET based sensor is an interesting approach for this because of (i) gate electrode of FET is embedded in the device and not electrically connected to the test solution and (ii) does not require a reference electrode. Regarding materials for FET fabrication, more recently nanostructured semiconductor MO_x materials with morphologies of nanoflowers, nanorectangles, nanowires, nanotubes have received great interest due to large-surface to volume ratio of the nanomaterials, advantageous for optimizing the sensing performance. Cheng et al. [180] reported a SnO_2 nanobelt based FET pH sensor (schematic representation is shown in Fig. 9d with an inset of SEM image of nanobelt) which shows sensitivity in the range of pH 5 to 8.5. Fig. 9e shows the real-time responses, the average channel conductance of a sensor in response to different pH values from 5.0 to 8.5 at ten different molar concentrations [180]. This change in conductance of the sensor with pH value of solution is due to the surface protonation/deprotonation on the SnO_2 nanobelt. It was found the SnO_2 nanorod (55.18 mV/pH) shows high sensitivity due to the high surface-to-volume ratio for the nanostructured material which provides larger surface sites and more effective sensing areas as compared to SnO_2 thin film (48.04 mV/pH) [68].

6.5. Titanium oxide (TiO_2) based pH sensors

Titanium oxide films are considered as good pH sensitive layers due to their high chemical stability. So far, different methods such as metal organic chemical vapour deposition (MOCVD) [62], sol-gel [61], anodization of Ti substrate [63], sputtering [144] etc. were used for the preparation of TiO_2 pH SE. Recently, researchers proposed a new approach for the sensitivity of TiO_2 nanotubes based pH sensor by irradiation with ultraviolet (UV) light/rays [63]. In this work, the fabrication of a pH sensor was carried out by by electrochemical anodization of titanium substrate electrode leading to formation of TiO_2 nanotube array. They found that the nanotube array significantly increases the electrode surface area and hence the modified Ti electrode with the amorphous TiO_2 nanotube array film shows good sensitivity. The oxidation time of the electrode changes the properties of the nanotube array and consequently pH sensitivity. Later, TiO_2 nanotube array film was irradiated with ultraviolet (UV) rays for improving electrode sensitivity [63]. After irradiation, the sensitivity was close to the theoretical Nernstian response. The UV irradiation improves the hydrophilic property of the electrode. They considered H^+ ion diffusion as the response mechanism of the pH sensor. The sensor was successfully tested for measurements of the pH of some drinks [63]. Chen et al. [182] developed a conductimetric pH sensor based on TiO_2/multiwall carbon nanotube (MWCNT)/cellulose hybrid nanocomposite. This sensor exhibited in the pH range of 1–12 two linear regions in the conductance dependence on pH. The large surface area of cellulose hybrid nanocomposite increases the number of adsorption sites for H_3O^+ ions and hence increases the pH sensitivity [182].

In an EGFET based pH sensor, the gate must be a high conductivity material to serve as pH sensitive layer. However, TiO_2 possesses high sheet resistance because of its intrinsic property. So, for increasing the conductivity of TiO_2 either doping with metallic ions or modification of TiO_2 surface is necessary for the good sensing performance of TiO_2 based EGFET pH sensor. Chou and Chen [144] increased the conductivity of TiO_2 by doping with Ru metallic ions. They used co-sputtering method to develop Ru-doped TiO_2 as a sensing electrode of EGFET [144]. The fabricated sensor which showed excellent pH sensing performance is mentioned in Table 3. For decreasing cost and temperature, easy processing and increasing the conductivity of gate electrode of EGFET, Huang et al. [183] developed using hydrothermal method an EGFET pH sensor based on TiO_2 1D nanowire (NW) on a fluorine-doped tin oxide (FTO) substrate and compared the sensing performance with TiO_2 film [183]. Due to the higher surface to volume ratio and higher conductivity of NW TiO_2 this sensor exhibited better sensitivity (62 mV/pH; 0.064 mA/pH) than the sensitivity (50 mV/pH; 0.051 mA/pH) of TiO_2 film based pH sensor [183]. The higher conductivity of TiO_2 NWs is due to the lack of crystalline boundary along each NW and hence the presence of a larger number of oxygen related bonding sites for pH sensing. Moreover, the higher conductivity of TiO_2 NWs allows for better gate control than for TiO_2 film. It was observed that both devices exhibit a linear I_{DS}–pH relationship in the range of pH 2–12 [183].

Shin [62] reported the pH sensing performance of TiO_2 sensitive layer which was prepared by MOCVD method. In this work, investigated the pH sensing by capacitance-voltage measurement for electrolyte/insulator/silicon structures such as TiO_2/SiO_2/Si/Al and TiO_2 films which were annealed in the temperature range of 700–1000 °C [62]. Shin [62] observed that as-deposited films

showed a sensitivity of 57.2 mV/pH. However, the best sensitivity and long term stability were found for the film annealed at 900 °C and the fabricated sensors had no light induced drift. Liao and Chou [61] have studied the pH sensing performance of thin film TiO_2 coating prepared by sol-gel method, and the modified TiO_2 film used for drug sensitive membrane. TiO_2 film was immobilized by using phosphotungstic acid and polyvinyl chloride (PVC) to develop a procaine drug sensor, where TiO_2 thin film was utilized as a drug sensitive membrane substrate. They observed that the sensitivity of TiO_2 pH electrode was close to Nernstian response and the sensor exhibits low drift rate [61]. The fabricated procaine drug sensor exhibited a sensitivity of 55.03 $mVpC^{-1}$ with a response time of 16 s [61]. We fabricated a thick film interdigitated TiO_2 based conductimetric pH sensor along with portable AD5933, based impedance analyzer for characterization of the sensor in frequency range of 5–20 kHz [24,184]. The device is designed to enable the portable and autonomous operation for in-situ measurements as well as laboratory characterization of the sample. We observed that the electrical parameters of the TiO_2 based sensor are strongly dependent on the pH of solution in the low frequency range and from RC equivalent circuit it was observed that charge transfer and ion exchange are the two major phenomena for the sensing performances of a TiO_2 pH sensor.

6.6. Tungsten oxide (WO_3) based pH sensors

The transition metal oxide WO_3 is a promising hydrogen sensitive material used for measuring pH over a wide range. WO_3 has been used for constructing micro-electrochemical pH sensors for different applications [185]. WO_3 is a low cost and commonly available material with improved stability. The associated ease of morphological and structural control of the synthesized WO_3 nanostructures, reversible change of conductivity, selectivity, high sensitivity and biocompatibility makes them suitable for biomedical applications [72]. In 1987 Natan et al. reported for the first time WO_3 based microelectrochemical transistor pH sensor in which the sensor was operating either electrically or chemically by changing the gate voltage or the pH value of the solution [185]. Zhang and Xu [73] promoted utilization of CNTs in electrochemical sensors and for the first time reported a pH sensor based on MO_x -multiwalled CNTs (WO_3/MWNT). Even though the fabricated sensor shows a sub-Nernstian response, it has excellent reproducibility, stability, anti-interference properties and potential for miniaturization [73]. They followed single phase interaction mechanism to explain the pH sensing mechanism of WO_3 based pH sensors.

Chiang et al. [143] studied the influence of temperature, hysteresis, and drift on characteristics of a WO_3 based pH ISFET sensor. They found that pH sensitivity increases with increasing temperature and the temperature coefficient is dependent on pH value. Hysteresis width depends on measurement loop time and path. The hysteresis increases with increasing loop time and for acidic solutions is smaller than for basic solutions. Furthermore, it was found that the drift rate increases exponentially with pH value [143]. Nowadays, there is demand for microelectrochemical pH sensors, especially miniaturized and reliable pH sensors for physiological applications, such as cell determination. Yamamoto et al. [74] fabricated a W/WO_3 ultramicrosensor for monitoring of pH value of cultured endothelial cells and observation of the pH variation generated by normal, damaged and recovered endothelial cells. For wearable healthcare application, flexible WO_3 based pH sensors have potential applications due to their biocomptability. Recently, WO_3 based pH sensors (area of 1 mm^2) were fabricated on polyamide substrate (fabrication steps shown in Fig. 10a) which exhibit excellent sensitivity (-56.7 ± 1.3 mV/pH) in pH range 5–9, useful for monitoring physiological fluids [72]. The sensors show reversible performance (as presented in Fig. 10b) and a low reduction of 11.6% between the 1st and 3rd cycle. This decrease in sensitivity is due to the reactions at the electrode surface and charge sites saturation that occurs after long measurement [72].

6.7. Zinc oxide (ZnO) based pH sensors

The diverse beneficial properties of various nanostructured materials - nanorods, nanowires and nanotubes have attracted interest of researchers due to their potential application for the pH sensor fabrication [186–190]. Among these, ZnO-based nanostructured materials received great attention because of their electrochemical and biocompataible properties. The large surface area of ZnO nanostructures makes them more attractive for chemical, gas detection and biosensor applications [187–189]. Kang et al. [188] reported nanorods integrated with microchannel for pH measurement for investigating the change in conductance of the ZnO nanorods with variations of the pH in electrolyte solutions. In this work, ZnO nanorods exhibit a linear change in conductance being 8.5 nS/pH in the pH range 2–12 in the dark and 20 nS/pH when illuminated with UV light [188]. Batista and Mulato [191] used the sol-gel process (based on hydrolysis and polycondensation reactions) to develop ZnO EGFET pH sensors. As compared to crystalline ZnO, amorphous ZnO (film deposited at 150 °C) based EGFET shows a comparatively good sensitivity (38 mV/pH). The reason for this effect may be that pure and amorphous ZnO material would increase the number of surface sites (Ns from eq. (3)) leading to better sensing performance [191].

The various nanostructures of ZnO, such as nanorods, nanowires and nanotubes, have various influence on pH sensing performance. Fulati et al. [78] developed a new pH sensor based on ZnO nanotubes and compared its pH sensing performance with that of nanorod structures. They found that ZnO nanotubes provide sensitivity (45.9 mV/pH) two times greater than the sensitivity (28.4 mV/pH) of ZnO nanorods in the pH range 4–12. Fulati et al. [78] suggested that this difference in sensitivity occurs because ZnO nanotubes of low dimensionality have higher levels of surface and subsurface oxygen vacancies and provide large effective surface area with higher surface-to volume ratio as compared to ZnO nanorods. The difference in surface charge distribution at two walls of the metal oxide-electrolyte interface for ZnO nanorods and nanotubes in the $CaCl_2$ electrolyte is shown in Fig. 10c and d, respectively [78]. ZnO nanotubes and nanorods are more stable for pH close to 7 and dissolve much faster when pH is deviating from the neutral value. Therefore, such sensors are more useful for biological fluids [78]. A detailed investigation on the mechanism of pH-sensing using ZnO nanorods, with an emphasis on the nano-interface mechanism was described by Hilli and Magnus [148].

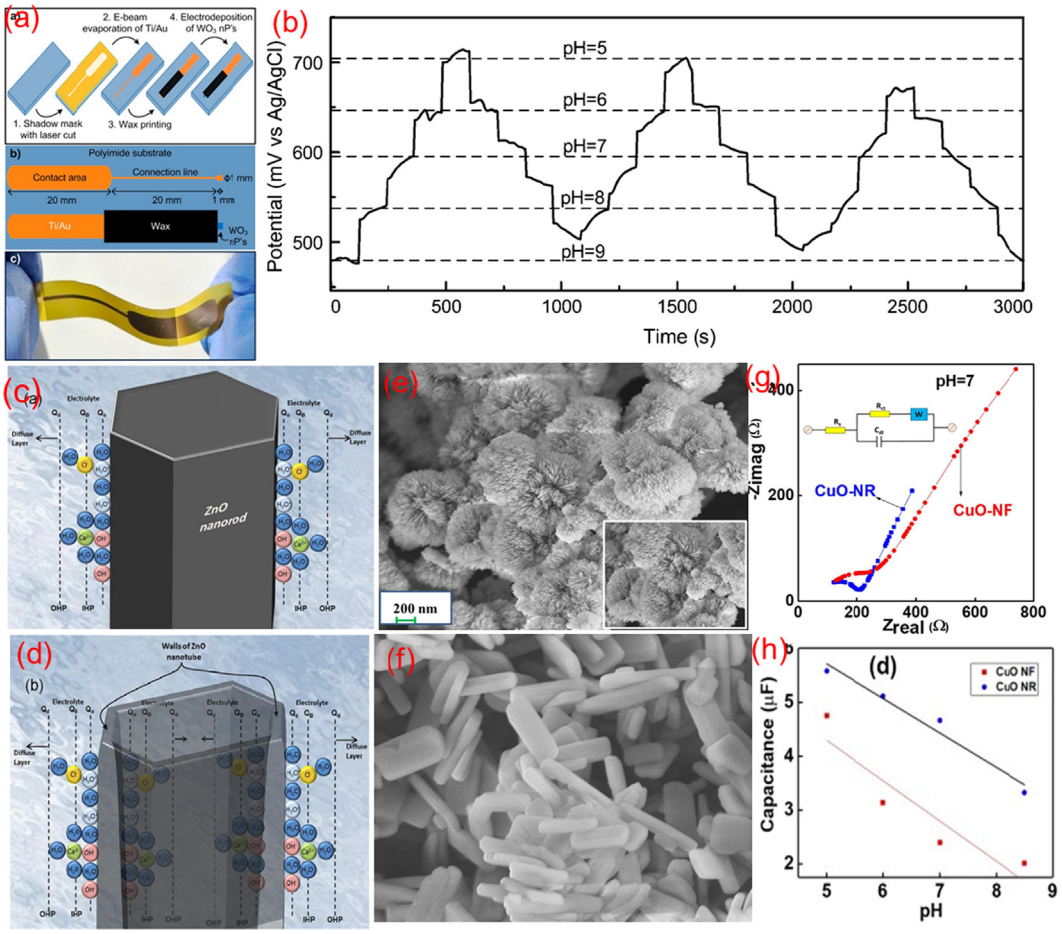

Fig. 10. (a) Schematic sensor fabrication (top), sensor design and structure (middle) and photograph of the final flexible WO_3 based sensor (bottom) *"Reprinted (adapted) with permission from* [72] *copyright (2014) American Chemical Society."* (b) Potential response of the pH sensor during three complete cycles in the range of pH 9–5 and 5–9 *"Reprinted (adapted) with permission from* [72] *copyright (2014) American Chemical Society.".* (c)–(d) Schematic representation of the surface charge distribution at the ZnO-electrolyte interface ZnO nanorods and ZnO nanotubes *with permission from* [78]. (e) – (f) FESEM images of CuO nanoflower (NF), and CuO nanorectangle (NR) "*Reprinted from Publication* [25] *with permission from Elsevier".* (g) Nyquist plot for CuO NR and CuO NF at pH 7 (inset shows the equivalent circuit) *"Reprinted from Publication* [25] *with permission from Elsevier".* (h) *the change in capacitance of the flexible CuO pH sensor in the region of* pH *5–8.5 for CuO NR and NF at 50 Hz. Reprinted from Publication* [25] *with permission from Elsevier".*

The nontoxicity and biocompatibility of ZnO received great attention for miniaturized sensors for biomedical application. Chiu et al. [192]. reported that the dangling bonds and surface states density induced on the surface of ZnO thin-film and the sidewall surface of the ZnO nanorod array may cause the Fermi level pinning effect and due to this effect the sensing parameters could not be effectively changed with the pH value solution of EGFET based pH sensor. In order to suppress the influence of Fermi level pinning, authors employed photoelectrochemical method to passivate the ZnO thin-film and the sidewall surface of ZnO nanorod array. As a result, i-ZnO (intrinsic- ZnO) nanorod array (further increased the sensitivity to 49.35 mV/pH from the value of 44.01 mV/pH for unpassivated i-ZnO nanorod [192]. Similarly, for ZnO unpassivated film has sensitivity of 38.46 mV/pH and for passivated film the sensitivity is 42.37 mV/pH [192].

6.8. CuO based pH sensor

Among nanostructured p-type semiconductor materials, CuO received a prominent position for multi-sensing applications, such as glucose, pH and gas sensors [25,193–196]. In addition, CuO also found applications in photodetectors, solar cells, supercapacitors and batteries, due to its high surface to volume ratio which enhances the sensitivity, selectivity, catalytic activity and its unique electrical and electrochemical properties [197–203]. The possibility of promoting electron transfer at a low potential, ease of synthesis and preparation of different nanostructures, shapes and dimensions, and environmentally friendly nature are advantages of this material in electrochemical applications [204]. The electrochemical properties of CuO are strongly dependent on morphologies because of different specific surface areas. Numerous methods have recently been reported to synthesize various CuO nanostructures

with different morphologies (1D, 2D and 3D) such as nanoparticles, nanotubes, nanoflowers nanoribbons, nanoleaves, nanorods, etc. by using various chemical and physical methods [196,202–207]. However, limited studies were carried out to investigate the pH sensing performance of these CuO nanomaterials. Zaman et al. [207] reported that CuO nanoflowers (NF) exhibited sub-Nernstian response of 28 mV/pH in the range of pH 2–11. We observed that the surface morphology influences (FESEM imags of CuO NF and CuO nanorectangles (NR) are shown in Fig. 10e and f) the charge transfer phenomena of the MO_x–solution interface and hence the sensor performance, as confirmed by the EIS studies (Fig. 10g) [25]. The CuO nanorectangle based sensors have better stability with respect to CuO nanoflowers based sensor. It was observed that the CuO nanorectangle based sensor exhibits a sensitivity of 0.64 μF/pH in the range of pH 5–8.5 (shown in Fig. 10h). For wearable applications, the flexible CuO nanorectangle based pH sensor shows negligible interference to other ions and analytes, such as Na^+, K^+, glucose, and urea [25].

6.9. Yttria stabilized zirconia (YSZ) based pH sensors

In the past few decades, there has been more concentration on measuring the pH of aqueous solutions at high temperature and high pressure, especially in applications involving nuclear power, geothermal energy, fossil power, oil well drilling, scale deposition, crystal growth, corrosion and hydrometallurgy [208,209]. Initially, the major works in this area were focused on hydrogen concentration cells and palladium hydride electrodes. However, use of these pH measurement devices is limited to the systems that are stable against the reduction by hydrogen and these sensors cannot be used for monitoring of pH of the high temperature aqueous systems containing oxidizing species. Niedrach [210] developed a promising material, YSZ membrane sensor for high-temperature potentiometry. Mcdonald et al. [209] used YSZ based pH sensor which obeyed Nernstian behavior for measurements up to 300 °C. Seneviratne et al. [211] reported a flow-through electrochemical cell with a flow through yttria-stabilized zirconia sensor and a flow through external reference electrode which was used for the first time for measuring pH at 250 °C in process sulfate systems relevant to hydrometallurgical process of nickeliferous laterites [211]. YSZ sensors are often applied in geothermal situations, like the acidic gases emanating from a volcano, and for nuclear power devices, especially nuclear waste disposal sites.

6.10. CeO_2 based pH sensors

Betelu et al. [212] reported the fabrication of CeO_2 based screen printed pH SE and its application for continuous pH measurement of the pore water in the Callovo-Oxfordian formation (COx) during its evolution as a radioactive waste repository. Zr or Sm was substituted to CeO_2 for improving the sensitivity of the electrode. Potentiometric method was used for monitoring the pH of the pore water. The EIS studies of the SE showed that in the low frequency range the mass transport (diffusion-convection) occurs at the electrolyte/electrode interface. In the high frequency range, the response was attributed to the charge transfer phenomena [212]. These authors found that a Zr substituted CeO_2 sensitive electrode shows better sensitivity in the pH range of 5.5–13.5 at 25 °C than Sm substituted electrode and a single oxygen intercalation is responsible for the pH sensing mechanism of CeO_2 based sensor [212].

6.11. Lead oxide (PbO_2) based pH sensors

Lead Oxide is exploited in various electrochemical applications. The deficiency of oxygen or excess of lead in PbO_2 results in its characteristic metallic conductivity. In PbO_2 both the lead and the oxygen ions are involved in electrochemical reactions. Due to excellent electrochemical properties, lead oxide has been used for pH sensor fabrication. Eftekhari [213] reported the possibility of fabrication of two modified electrodes α-PbO_2 and β-PbO_2 on aluminum substrate electrode for pH measurements. The aluminum substrate electrode helps to improve the stability and growth of the electroactive film. These electrodes are also used for the measurement of pH during flow injection analysis and measurement of pH of some real samples, like soft drinks and fruit juices [213]. Razmi et al. [214] presented α-PbO_2 and β-PbO_2 on a carbon ceramic electrode for pH measurements. The electrochemical properties of the PbO_2 film were improved by using the carbon composite electrode. The fabricated sensors are very suitable for measuring the pH of natural samples. The PbO_2 sensing film coated on carbon ceramic electrode shows excellent response time, high selectivity, good stability and long term usage [214].

6.12. Lithium lanthanum titanate based pH sensor

Bohnke et al. [96] explored the use of high lithium conductive perovskite compound lithium lanthanum titanate (LLTO) as a pH sensor. The authors tried to investigate the mechanism of pH detection of LLTO based sensors by using impedance spectroscopicanalysis [96]. The pH sensor based on LLTO found applications in the food industry [215]. Even though it does not follow the Nernstian response, it shows good sensitivity and response time. The authors followed two methods for the preparation of ion selective electrode and electrochemical cell, comprising membrane configuration with liquid or solid internal reference [216]. Vijayakumar et al. [217] prepared LLTO pH sensor by solid state reaction and sol-gel method. According to them, in the solid state reaction method small grain size of the powder is favorable for proper pH sensitivity and the sensitivity increases when the LLTO powder is ground before heat treatment. Moreover, compared to the solid state method, sol-gel reaction requires much less time for powder preparation and permits to obtain pure and high quality LLTO [217].

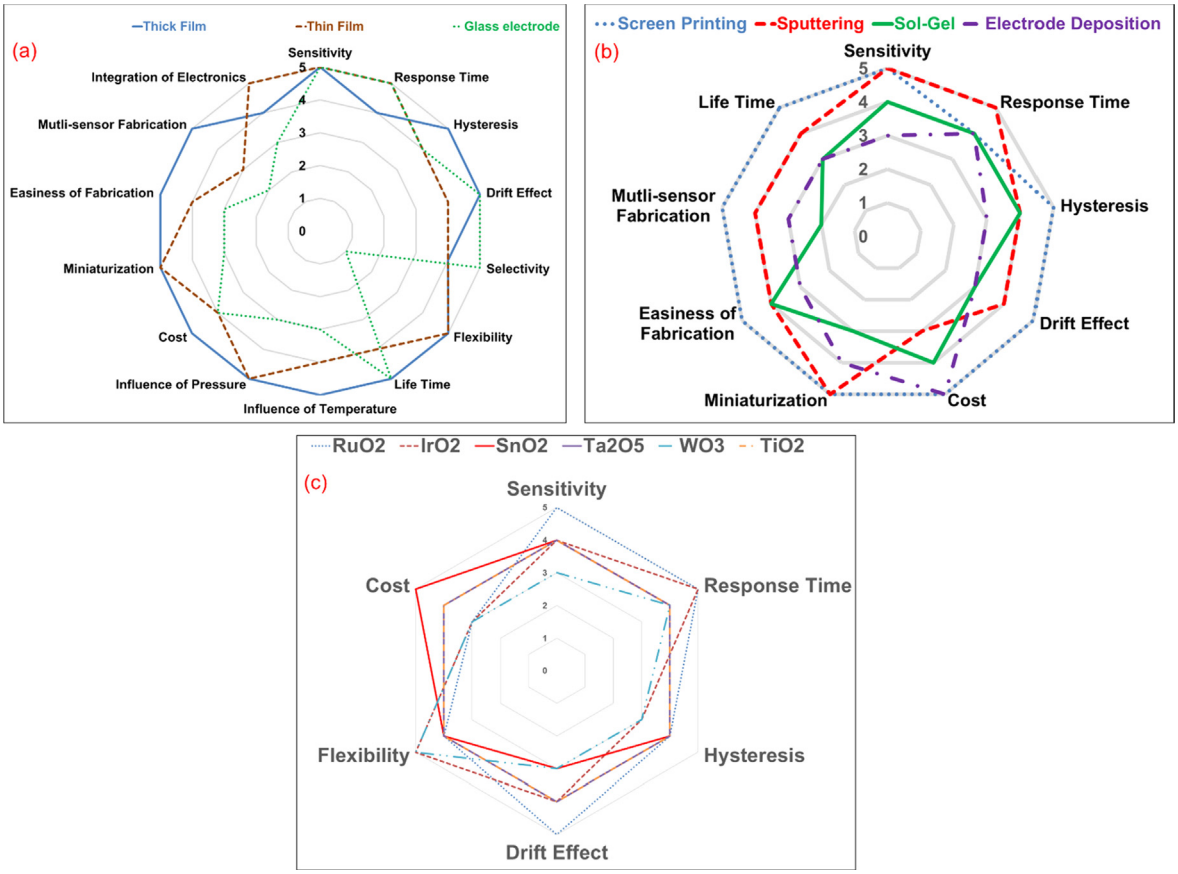

Fig. 11. Comparison of properties and pH sensing performance based on (a) type of electrode (b) method of fabrication and (c) different MO_x compositions Challenges and future perspectives.

6.13. Other MO_x based pH sensors

In addition to the materials described above there are some works concerning the fabrication of pH sensors by using other oxides: MnO_2 [218,219], cobalt oxide [220,221], molybdenum bronzes [222], NiO [223], $Ni_3(PO_4)_2{\cdot}8H_2O$ nano/microflakes layer on nickel foam (NF) [224], $CeTi_xO_y$ film [225], manganese oxide nanoparticles electrodeposited on graphenized pencil lead electrode [226], indium tin oxide (ITO [134]), etc. We presented here only some important materials which are widely used for pH sensor fabrication.

7. Comparison of pH sensing performance of MO_x sensors

This review demonstrated that the sensing performance of the MO_x based pH sensors is influenced by many factors including fabrication process, and material properties. Form the investigation we observed that the major approaches reported in literature for the fabrication of MO_x pH sensors are: screen printing, sputtering, sol-gel, carbonate melt oxidation, electrodeposition, chemical vapor deposition, and Pechini method, etc. The pH sensing performance of various MO_x sensors is shown in Fig. 11, where a comparison of some selected features, applicability, cost and sensing performance of pH sensors with metal oxide electrodes are schematically illustrated. In Fig. 11a, some characteristic properties of thick film, thin film and glass electrode based pH sensors are compared. It was observed that in comparison with glass and thin film based pH sensors, the thick film based pH sensors have many advantages for future applications in terms of fabrication of multi-sensors on a single substrate, fabrication of compatible RE with easy fabrication, low cost of fabrication along with excellent sensing performance. The parameters of pH sensors fabricated by different methods are illustrated in Fig. 11b. The screen printing method offers many advantageous properties (described in Fig. 11b). The nanostructure of the material influences the response time of the sensor. Thin film based deposition method can enable tuning the nanostructure of the material and can lead to a faster response than for thick film based pH sensors. A comparison of the sensing performance and the cost of most widely used MO_x based pH sensors are shown in Fig. 11c. The sensing performance of each material is strongly influenced by the method of fabrication and structure of the material. Comparison of the average sensitivities of various materials shows that RuO_2 based sensors have very good sensing performance even though the cost of these materials is high.

Even though many remarkable advances have been reported in the MO_x based pH sensors, many challenges remain for development of pH sensors, especially concerning different applications such as biomedical, food and water quality monitoring. The major

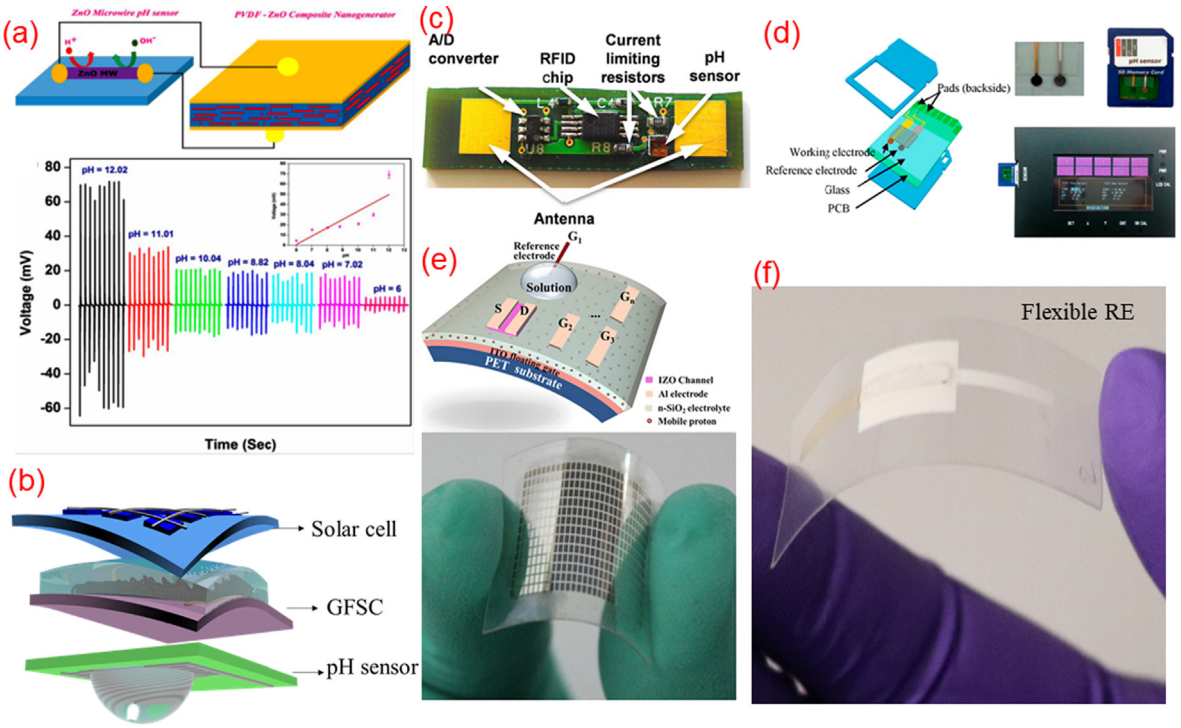

Fig. 12. Demonstration of (a) self-powered pH sensors, based on a ZnO microwire sensor and a hybrid composite nanogenerator with an output results [230], (b) 3D schema of FSPP (flexible PV cell, GFSC and pH sensor *with permission* [3]. (c) Passively powered, implantable RFID tag pH sensor prototype *with permission from* [89] (d) integrated pH sensor with thin-film Ag/AgCl reference electrode coated with Graphene Oxide (GO) and pH working electrode on glass substrate, packaged in an SD card with laboratory-made potentiometer *with permission from* [231]. (e) Schematic representation of the flexible pH sensor based on an IZO neuromorphic transistor with multiple gate electrodes with image of the sensor array fabricated on a flexible PET substrate, *with permission from* [41] (f) Image of flexible Ag/AgCl/KCl based RE fabricated on PET substrate by screen printing method *with permission from* [103].

design and development efforts in the field are focused on flexible, wearable, portable, miniaturized sensors for online monitoring applications. Some of new advances in pH sensing technology based on metal oxides, full measurement systems and compatible REs are summarized in Fig. 12. These include a ZnO based self-powered flexible pH sensor [230], shown in Fig. 12a, self-powered pH sensor using energy autonomous system (shown in Fig. 12b) [3], RFID tag pH sensor based on CNT chemi-resistor for wireless application (shown in Fig. 12c) [89], a miniaturized pH sensor based on thin film of Ag/AgCl RE and IrO_2 SE packaged in an SD card (shown in Fig. 12d) [231], a flexible electrolyte-gated neuron transistor with amorphous oxide (IZO-Indium Zinc Oxide) channel layers for biochemical pH sensing applications (shown in Fig. 12e) [41], disposable Ag/AgCl RE prepared on paper substrate by screen printing [232] and flexible Ag/AgCl/KCl based RE fabricated by screen printing method (presented in Fig. 12f) [103].

To address the emerging challenges, one of the future directions will be using proper sensitive materials for electrochemical MO_x pH sensors to make them suitable for applications such as food processing, environmental monitoring and biomedical applications, etc. Concerning materials and design of sensors the major challenges are toxicity of materials, cost, flexibility and bendability of materials, integration of SE and RE on single substrate for potentiometric sensors miniaturization. Among others, the cost-effective fabrication, choice of substrates, and easy integration of sensors are some of the important issues to be considered. The scope of some future and potential solutions as well as current challenges are described below. The major drawback in majority of metal oxide based sensors is their slow response in neutral and basic solutions. This need to be overcome because the major application field of sensors lies in the pH range of 5–10. One of the alternative method is to mix metal oxide with conductive material; in such case the conductive material will act as a path of ion transfer. The electrochemical double layer formation in conductive element (for example, graphite) and pesuodocapacitance of MO_x will collectively involve in the electrochemical reactions.

7.1. Water quality monitoring

As an alternative to traditional glass based pH sensors, RuO_2 based pH sensors received promising attention in water quality monitoring due to its high sensitivity and chemical stability for a long period. However, the higher cost and low sensitivity in basic solution hinders the use of RuO_2 in many practical applications. The issues related to RuO_2 based electrodes are being addressed with mixed oxides or doped oxides. Another option is SE based on ceramic materials [233,234] such as doped or undoped ZrO_2 [235]. However, there are not many studies focused on ceramic materials, for example, Pb-free perovskites for pH-SEs. An interesting

alternative is also application of LTCC technology for fabrication of pH sensors with sensitive SE based on ceramic materials. The major advantages of this technology are (i) using cheap and simple screen printing method for deposition of sensing and reference electrodes (ii) possibility of integration in a LTCC substrate passive components for wireless application, e.g. for online monitoring of water pollution, and (iii) advances in sensor miniaturization and reliability. For realization of this purpose, a challenging task is preparation of an Ag/AgCl RE compatible with LTCC substrate. In previous works [23], preparation of glass-KCl composition functioning as a salt bridge seemed to be a crucial obstacle in RE fabrication. It can be overcome by using the possibilities of different glass-KCl compositions which are compatible with LTCC substrate. Such sensors have a significant application potential for multi-sensors and water pollution monitoring systems and aquaculture [236–238].

7.2. Food quality monitoring

In the food processing plant, “non-glass” pH sensors have great importance to ensure the quality of food. For example, in the meat industry, it is difficult to insert glass electrodes inside the meat because of possible breaking of the glass. In such case, pH sensors on alumina substrate should be very useful. Sensitive materials based on nanostructured ZnO, Ta_2O_5 or SnO_2 will be advantageous due to their biocompatibility and high sensitivity. These materials will also be suitable for fabrication of flexible pH sensors which can be disposable. For food quality monitoring sensors, during the fabrication and characterization of sensors it is necessary to consider the influence of the fatty acids or other proteins particles present in the food. Flexible pH sensor on a food package with embedded RFID tags and communication system can predict the quality of food for producers and consumers.

7.3. Wearable biosensors for medical application

The electrochemical biosensors provide a simple and attractive way for analyzing the biological samples (sweat, urine, tears) through direct measurement of electrochemical reactions [239]. The monitoring of pH value of skin is important to detect pathogenesis of skin diseases like irritant contact dermatitis, acne vulgaris, atopic dermatitis, etc. [240,241] The pH of skin is related to pH of sweat [242,243]. Moreover, the continuous monitoring of pH value of blood and brain tissue is very important for the patients who have suffered stroke and traumatic brain injury. In addition, one of the greatest achievements in potentiometric pH sensors is the fabrication of novel wearable pH sensors for real time monitoring of pH changes in a wound. Hence, the development of new sensing biocompatible materials and designs is of fundamental importance in flexible electrochemical sensors for healthy life. The flexible or wearable pH sensors have great importance for early stage determination of many chronic diseases. For example, the diabetic patient’s simultaneous changes in level of pH and glucose effect the body metabolism. Hence, for better performance and selectivity of the sensor, flexible multi-sensor patches, which consist of glucose, temperature and other dissolved ions monitoring electrodes on a single substrate, may be useful for sweat analysis [244,245]. Flexible RFID with electronics wireless communication will be advantageous for online monitoring sweat and we show this in our recent graphite based pH sensor [4]. Ink jet printing or screen printing method can be the right approach for electrode fabrication for such sensors. For long term applications, nanostructured or doped ZnO, SnO_2 or TiO_2 inks and pastes will be suitable for sensitive electrode fabrication. For on body monitoring, a sensor printed on clothes or tattoo may be useful wearable application. Flexible triboelectric nanogenerator [246] for power supply to the electronic part which can be integrated with the wearable sensor will be helpful for online monitoring.

Until now, few MO_x have been used for the construction of the electrochemical flexible pH sensors. The major MO_x materials reported for flexible, disposable and wearable sensors included IrO_2 [40,247], RuO_2 [160,248], ZnO [77], ITO [249], IZO [41] and WO_3 [72]. Synthesis of new nanostructured materials and implementation of novel designs are necessary for the further development of electrochemical pH sensors. More works should be carried out for IGZO (Indium Gallium ZnO) and GTZO (Ga- Sn- ZnO) based sensitive materials for flexible pH sensor applications. IGZO [250] shows good pH sensing and very good performance for thin film transistor applications. Sol-gel method may be one of the best options for the preparation of low cost nanostructured sensitive materials for large area of flexible devices. The major problem of this method is the deposition of MO_x on a flexible polymer or paper based substrate at low temperature. Self-energy generating combustion method of material preparation can overcome this issue [251]. It enables developing transparent conductive oxide based thin large-area, low-cost electronics for sensor arrays. The fabricated sensors can be integrated into textile, tattoo, skin, wrist watches, bandages, etc. Another interesting approach is the preparation of nanoparticle growth on the surface of a substrate for single molecule determination of biological samples. The morphologies based on nanotubes, and nanorectangles should be very interesting due to large surface area for detecting the particles. For transferring the nano morphological samples on the top of flexible substrate tactile printing or contact printing methods should be promising approaches. We recently reported a flexible capacitive sensor for energy autonomous application, prepared by transfer printing method [252] and nanostructures fabricated by contact printing method [253,254].

7.4. Extreme environment applications

For applications at high temperature, high pressure and in aggressive chemical environment (e.g. in nuclear respiratory systems), LTCC based pH sensors seem to be well fitted. Doped or undoped CeO_2 and ZrO_2 [255] based sensors are well fitted for high temperature applications. Preparation of new co-firable pastes based on these compounds for LTCC technology may be a good approach for a new pH sensor design. To overcome the issue of RE, differential electrode prepared on the same substrate by screen printing method [248] may be a good attempt for RE fabrication instead of Ag/AgCl RE. Moreover, instead of potentiometric pH sensors, IDE based conductimetric pH sensors can be a better alternative. However, the major practical limitation of IDE based pH

sensors is the strong influence of the solution conductivity and degradation of materials. This problem can be overcome by using high dielectric materials or perovskite-based composites as SEs and suitable dimensions of IDE, as well as by measurement of conductivity by a sensor integrated with the pH sensor. In high and low temperature application of the sensor, the sensitivity and standard potential values are changing with temperature [256]. Thus, for future online monitoring applications of pH sensors it is necessary to ensure integration of electronic parts and control the changes of potential with temperature to minimize its influence on sensing performance.

7.5. Energy autonomous sensors

Power requirement for operating the sensors for online monitoring is a critical challenge. The chemi-reistive, ISFET based sensors require an operating potential. Moreover, the electronic circuits for online data transfer and storage also require suitable power sources. The bulky battery has many disadvantages in such application, including heating, toxicity, life cycle, frequent charging, etc. To overcome these challenges, energy autonomous sensors combining integration of energy generator (for example solar cell) and storage (for example supercapacitor) with the sensors and electronic components will have tremendous application in online monitoring. In our previous work [3,118,257], we used flexible solar cell and supercapacitor as power pack for voltage source to sensors for wearable application and also for water quality monitoring by integrating with robotic fish [258,259]. Further improvement is needed for the wireless application. The energy is required to deliver power for the electronic circuits and for remote applications including those in extreme environmental conditions. New strategies are demanded in this field, similar to those used for other applications.

8. Conclusion

The increasing demand for reliable sensors for online monitoring focuses the pH sensors based research on fabrication of metal oxides MO_x. Such sensors, including those fabricated using thin and thick film techniques, have been gaining significant importance in current electrochemical sensing technology. This paper presented an overview of the fabrication methods, measurement techniques and the sensing performances of widely used MO_x based pH sensors. Major techniques employed to provide the information about the sensing mechanism of MO_x based pH sensors were also described. With fast responses, wider pH sensing range, excellent sensitivity, easy integration with microelectronic components, wearable structural compatibility, biocompatibility, ability to integrate with clothes, paper, skin, etc., the MO_x based pH sensors offer a number of advantages over glass based sensors. In the present review, the development perspectives for MO_x based pH sensors were demonstrated including flexible devices for online or in vivo biomedical applications, food quality monitoring and environmental monitoring.

Acknowledgements

The work was partly supported by the Engineering and Physical Sciences Research Council (EPSRC) through Engineering Fellowship for Growth - PRINTSKIN (EP/M002527/1) and neuPRINTSKIN (EP/R029644/1) and European Commission through AQUASENSE (H2020-MSCA-ITN-2018-813680) and North West Centre for Advanced Manufacturing (NW CAM) project supported by the European Union's INTERREG VA Programme (H2020-Intereg-IVA5055), managed by the Special EU Programmes Body (SEUPB). The views and opinions in this document do not necessarily reflect those of the European Commission or the Special EU Programmes Body (SEUPB).

References

[1] Guinovart T, Valdés-Ramírez G, Windmiller JR, Andrade FJ, Wang J. Bandage-based wearable potentiometric sensor for monitoring wound pH. Electroanalysis 2014;26:1345–53.
[2] Zhuiykov S. Solid-state sensors monitoring parameters of water quality for the next generation of wireless sensor networks. Sens Actuat, B 2012;161:1–20.
[3] Manjakkal L, Núñez CG, Dang W, Dahiya R. Flexible self-charging supercapacitor based on graphene-Ag-3D graphene foam electrodes. Nano Energy 2018;51:604–12.
[4] Dang W, Manjakkal L, Navaraj WT, Lorenzelli L, Vinciguerra V, Dahiya R. Stretchable wireless system for sweat pH monitoring. Biosens Bioelectron 2018;107:192–202.
[5] Bandodkar AJ, Hung VW, Jia W, Valdés-Ramírez G, Windmiller JR, Martinez AG, et al. Tattoo-based potentiometric ion-selective sensors for epidermal pH monitoring. Analyst 2013;138:123–8.
[6] Kim J, Cho TN, Valdés-Ramírez G, Wang J. A wearable fingernail chemical sensing platform: pH sensing at your fingertips. Talanta 2016;150:622–8.
[7] Paek K, Yang H, Lee J, Park J, Kim BJ. Efficient colorimetric pH sensor based on responsive polymer–quantum dot integrated graphene oxide. ACS Nano 2014;8:2848–56.
[8] Cao H, Landge V, Tata U, Seo Y-S, Rao S, Tang S-J, et al. An implantable, batteryless, and wireless capsule with integrated impedance and pH sensors for gastroesophageal reflux monitoring. IEEE Trans Biomed Eng 2012;59:3131–9.
[9] Ravi PP, Lindner J, Oechsner H, Lemmer A. Effects of target pH-value on organic acids and methane production in two-stage anaerobic digestion of vegetable waste. Bioresour Technol 2018;247:96–102.
[10] Lonsdale W, Wajrak M, Alameh K. Manufacture and application of RuO_2 solid-state metal-oxide pH sensor to common beverages. Talanta 2018;180:277–81.
[11] Lian Y, Zhang W, Ding L, Zhang X, Zhang Y, Wang XD. Nanomaterials for intracellular pH sensing and imaging. Novel Nanomaterials for Biomedical, Environmental and Energy Applications: Elsevier. 2019. p. 241–73.
[12] Han J, Cui D, Li Y, Zhang H, Huang Y, Zheng Z, et al. A gastroesophageal tract pH sensor based on the H + -ISFET and the monitoring system for 24 h. Sens Actuat, B 2000;66:203–4.
[13] Kohn DH, Sarmadi M, Helman JI, Krebsbach PH. Effects of pH on human bone marrow stromal cells in vitro: Implications for tissue engineering of bone. J Biomed Mater Res 2002;60:292–9.

[14] Srivastava J, Barber DL, Jacobson MP. Intracellular pH sensors: design principles and functional significance. Physiology 2007;22:30–9.
[15] Curto VF, Fay C, Coyle S, Byrne R, O'Toole C, Barry C, et al. Real-time sweat pH monitoring based on a wearable chemical barcode micro-fluidic platform incorporating ionic liquids. Sens Actuat, B 2012;171–172:1327–34.
[16] Gibson AM, Bratchell N, Roberts T. Predicting microbial growth: growth responses of salmonellae in a laboratory medium as affected by pH, sodium chloride and storage temperature. Int J Food Microbiol 1988;6:155–78.
[17] Kress-Rogers E. Solid-state pH sensors for food applications. Trends Food Sci Technol 1991;2:320–4.
[18] Stippl V, Delgado A, Becker T. Development of a method for the optical in-situ determination of pH value during high-pressure treatment of fluid food. Innov Food Sci Emerg Technol 2004;5:285–92.
[19] Uria N, Abramova N, Bratov A, Muñoz-Pascual F-X, Baldrich E. Miniaturized metal oxide pH sensors for bacteria detection. Talanta 2016;147:364–9.
[20] Atkinson JK, Cranny A, Glasspool WV, Mihell JA. An investigation of the performance characteristics and operational lifetimes of multi-element thick film sensor arrays used in the determination of water quality parameters. Sens Actuat, B 1999;54:215–31.
[21] Gupta VK, Jain CK, Ali I, Sharma M, Saini VK. Removal of cadmium and nickel from wastewater using bagasse fly ash—a sugar industry waste. Water Res 2003;37:4038–44.
[22] Martínez-Máñez R, Soto J, García-Breijo E, Gil L, Ibáñez J, Gadea E. A multisensor in thick-film technology for water quality control. Sens Actuat, A 2005;120:589–95.
[23] Manjakkal L, Zaraska K, Cvejin K, Kulawik J, Szwagierczak D. Potentiometric RuO_2–Ta_2O_5 pH sensors fabricated using thick film and LTCC technologies. Talanta 2016;147:233–40.
[24] Simić M, Stojanović GM, Manjakkal L, Zaraska K. Multi-sensor system for remote environmental (air and water) quality monitoring. 2016 24th Telecommunications Forum (TELFOR). 2016. p. 1–4.
[25] Manjakkal L, Sakthivel B, Gopalakrishnan N, Dahiya R. Printed flexible electrochemical pH sensors based on CuO nanorods. Sens Actuat, B 2018;263:50–8.
[26] Dang W, Manjakkal L, Lorenzelli L, Vinciguerra V, Dahiya R. Stretchable pH sensing patch in a hybrid package. 2017 IEEE SENSORS. 2017. p. 1–3.
[27] Manjakkal L, Dang W, Yogeswaran N, Dahiya R. Textile-based potentiometric electrochemical pH sensor for wearable applications. Biosensors 2019;9:14.
[28] Nakata S, Arie T, Akita S, Takei K. Wearable, flexible, and multifunctional healthcare device with an ISFET chemical sensor for simultaneous sweat pH and skin temperature monitoring. ACS Sensors 2017;2:443–8.
[29] Anastasova S, Crewther B, Bembnowicz P, Curto V, Ip HMD, Rosa B, et al. A wearable multisensing patch for continuous sweat monitoring. Biosens Bioelectron 2017;93:139–45.
[30] Lee H, Choi TK, Lee YB, Cho HR, Ghaffari R, Wang L, et al. A graphene-based electrochemical device with thermoresponsive microneedles for diabetes monitoring and therapy. Nat Nanotechnol 2016;11:566.
[31] Korostynska O, Arshak K, Gill E, Arshak A. State key laboratory of nonlinear mechanics (LNM), institute of mechanics, chinese academy of sciences, Beijing 100080, China. Sensors 2007;7:3027–42.
[32] Yuqing M, Jianrong C, Keming F. New technology for the detection of pH. J Biochem Bioph Methods 2005;63:1–9.
[33] Qin Y, Kwon H-J, Howlader MMR, Deen MJ. Microfabricated electrochemical pH and free chlorine sensors for water quality monitoring: recent advances and research challenges. RSC Adv 2015;5:69086–109.
[34] Alam AU, Qin Y, Nambiar S, Yeow JTW, Howlader MMR, Hu N-X, et al. Polymers and organic materials-based pH sensors for healthcare applications. Prog Mater Sci 2018;96:174–216.
[35] Vonau W, Guth U. pH Monitoring: a review. J Solid State Electrochem 2006;10:746–52.
[36] Głab S, Hulanicki A, Edwall G, Ingman F. Metal-metal oxide and metal oxide electrodes as pH sensors. Crit Rev Anal Chem 1989;21:29–47.
[37] Kurzweil P. Metal oxides and ion-exchanging surfaces as pH sensors in liquids: state-of-the-art and outlook. Sensors. 2009;9:4955–85.
[38] Xu B, Zhang W-D. Modification of vertically aligned carbon nanotubes with RuO_2 for a solid-state pH sensor. Electrochim Acta 2010;55:2859–64.
[39] Zhuiykov S, Kats E, Kalantar-zadeh K, Breedon M, Miura N. Influence of thickness of sub-micron Cu_2O-doped RuO_2 electrode on sensing performance of planar electrochemical pH sensors. Mater Lett 2012;75:165–8.
[40] Huang W-D, Cao H, Deb S, Chiao M, Chiao JC. A flexible pH sensor based on the iridium oxide sensing film. Sens Actuat, A 2011;169:1–11.
[41] Liu N, Zhu LQ, Feng P, Wan CJ, Liu YH, Shi Y, et al. Flexible sensory platform based on oxide-based neuromorphic transistors. Sci Rep 2015;5:18082.
[42] Lonsdale W, Shylendra SP, Wajrak M, Alameh K. Application of all solid-state 3D printed pH sensor to beverage samples using matrix matched standard. Talanta 2019;196:18–21.
[43] Bishnoi SW, Rozell CJ, Levin CS, Gheith MK, Johnson BR, Johnson DH, et al. All-optical nanoscale pH meter. Nano Lett 2006;6:1687–92.
[44] Chan KWY, Liu G, Song X, Kim H, Yu T, Arifin DR, et al. MRI-detectable pH nanosensors incorporated into hydrogels for in vivo sensing of transplanted-cell viability. Nat Mater 2013;12:268.
[45] Marshall AJ, Blyth J, Davidson CAB, Lowe CR. pH-sensitive holographic sensors. Anal Chem 2003;75:4423–31.
[46] Wencel D, Abel T, McDonagh C. Optical chemical pH sensors. Anal Chem 2014;86:15–29.
[47] Bashir R, Hilt JZ, Elibol O, Gupta A, Peppas NA. Micromechanical cantilever as an ultrasensitive pH microsensor. Appl Phys Lett 2002;81:3091–3.
[48] Blair S, Lowe MP, Mathieu CE, Parker D, Senanayake PK, Kataky R. Narrow-range optical pH sensors based on luminescent europium and terbium complexes immobilized in a sol gel glass. Inorg Chem 2001;40:5860–7.
[49] Cai QY, Grimes CA. A remote query magnetoelastic pH sensor. Sens Actuat, B 2000;71:112–7.
[50] Shi W, Li X, Ma H. A tunable ratiometric pH sensor based on carbon nanodots for the quantitative measurement of the intracellular pH of whole cells. Angew Chem Int Ed 2012;51:6432–5.
[51] Taib MN, Andres R, Narayanaswamy R. Extending the response range of an optical fibre pH sensor using an artificial neural network. Anal Chim Acta 1996;330:31–40.
[52] Fog A, Buck RP. Electronic semiconducting oxides as pH sensors. Sensors Actuat 1984;5:137–46.
[53] Edwall G. Improved antimony-antimony (III) oxide pH electrodes. Med Biol Eng Compu 1978;16:661–9.
[54] Horton BE, Schweitzer S, DeRouin AJ, Ong KG. A varactor-based, inductively coupled wireless pH sensor. IEEE Sens J 2011;11:1061–6.
[55] Wang M, Yao S, Madou M. A long-term stable iridium oxide pH electrode. Sens Actuat, B 2002;81:313–5.
[56] Marzouk SAM, Ufer S, Buck RP, Johnson TA, Dunlap LA, Cascio WE. Electrodeposited iridium oxide pH electrode for measurement of extracellular myocardial acidosis during acute ischemia. Anal Chem 1998;70:5054–61.
[57] Prats-Alfonso E, Abad L, Casañ-Pastor N, Gonzalo-Ruiz J, Baldrich E. Iridium oxide pH sensor for biomedical applications. Case urea–urease in real urine samples. Biosens Bioelectron 2013;39:163–9.
[58] Liao Y-H, Chou J-C. Preparation and characteristics of ruthenium dioxide for pH array sensors with real-time measurement system. Sens Actuat, B 2008;128:603–12.
[59] Zhuiykov S. Morphology of Pt-doped nanofabricated RuO2 sensing electrodes and their properties in water quality monitoring sensors. Sens Actuat, B 2009;136:248–56.
[60] Manjakkal L, Cvejin K, Kulawik J, Zaraska K, Szwagierczak D, Socha RP. Fabrication of thick film sensitive RuO2-TiO2 and Ag/AgCl/KCl reference electrodes and their application for pH measurements. Sens Actuat, B 2014;204:57–67.
[61] Liao Y-H, Chou J-C. Preparation and characterization of the titanium dioxide thin films used for pH electrode and procaine drug sensor by sol–gel method. Mater Chem Phys 2009;114:542–8.
[62] Shin P-K. The pH-sensing and light-induced drift properties of titanium dioxide thin films deposited by MOCVD. Appl Surf Sci 2003;214:214–21.
[63] Zhao R, Xu M, Wang J, Chen G. A pH sensor based on the TiO_2 nanotube array modified Ti electrode. Electrochim Acta 2010;55:5647–51.
[64] Chou JC, Liao LP. Study of TiO2 thin films for ion sensitive field effect transistor application with RF sputtering deposition. Jpn J Appl Phys 2004;43:61–5.
[65] Tsai C, Chou JC, Sun TP, Hsiung SK. Study on the time-dependent slow response of the tin oxide pH electrode. IEEE Sens J 2006;6:1243–9.
[66] Chen P-Y, Yin L-T, Shi M-D, Lee Y-C. Drift and light characteristics of EGFET based on SnO_2/ITO sensing gate. Life Sci J 2013;10.

[67] Chin Y-L, Chou J-C, Sun T-P, Liao H-K, Chung W-Y, Hsiung S-K. A novel SnO_2/Al discrete gate ISFET pH sensor with CMOS standard process. Sens Actuat, B 2001;75:36–42.
[68] Li H-H, Dai W-S, Chou J-C, Cheng H-C. An extended-gate field-effect transistor with low-temperature hydrothermally synthesized SnO_2 nanorods as pH sensor. IEEE Electron Device Lett 2012;33:1495–7.
[69] Manjakkal L, Cvejin K, Bajac B, Kulawik J, Zaraska K, Szwagierczak D. Microstructural, impedance spectroscopic and potentiometric analysis of Ta_2O_5 electrochemical thick film pH Sensors. Electroanalysis 2015;27:770–81.
[70] Chen M, Jin Y, Qu X, Jin Q, Zhao J. Electrochemical impedance spectroscopy study of Ta_2O_5 based EIOS pH sensors in acid environment. Sens Actuat, B 2014;192:399–405.
[71] Kwon D-H, Cho B-W, Kim C-S, Sohn B-K. Effects of heat treatment on Ta_2O_5 sensing membrane for low drift and high sensitivity pH-ISFET. Sens Actuat, B 1996;34:441–5.
[72] Santos L, Neto JP, Crespo A, Nunes D, Costa N, Fonseca IM, et al. WO_3 nanoparticle-based conformable pH sensor. ACS Appl Mater Interfaces 2014;6:12226–34.
[73] Zhang W-D, Xu B. A solid-state pH sensor based on WO_3-modified vertically aligned multiwalled carbon nanotubes. Electrochem Commun 2009;11:1038–41.
[74] Yamamoto K, Shi G, Zhou T, Xu F, Zhu M, Liu M, et al. Solid-state pH ultramicrosensor based on a tungstic oxide film fabricated on a tungsten nanoelectrode and its application to the study of endothelial cells. Anal Chim Acta 2003;480:109–17.
[75] Lale A, Tsopela A, Civélas A, Salvagnac L, Launay J, Temple-Boyer P. Integration of tungsten layers for the mass fabrication of WO_3-based pH-sensitive potentiometric microsensors. Sens Actuat, B 2015;206:152–8.
[76] Chou J-C, Chiang J-L. Ion sensitive field effect transistor with amorphous tungsten trioxide gate for pH sensing. Sens Actuat, B 2000;62:81–7.
[77] Maiolo L, Mirabella S, Maita F, Alberti A, Minotti A, Strano V, et al. Flexible pH sensors based on polysilicon thin film transistors and ZnO nanowalls. Appl Phys Lett 2014;105:093501.
[78] Fulati A, Usman Ali SM, Riaz M, Amin G, Nur O, Willander M. Miniaturized pH sensors based on zinc oxide nanotubes/nanorods. Sensors 2009;9:8911–23.
[79] Al-Hilli SM, Willander M, Öst A, Strålfors P. ZnO nanorods as an intracellular sensor for pH measurements. J Appl Phys 2007;102:084304.
[80] Kao CH, Chen H, Lee ML, Liu CC, Ueng H-Y, Chu YC, et al. Multianalyte biosensor based on pH-sensitive ZnO electrolyte–insulator–semiconductor structures. J Appl Phys 2014;115:184701.
[81] Li H-H, Yang C-E, Kei C-C, Su C-Y, Dai W-S, Tseng J-K, et al. Coaxial-structured ZnO/silicon nanowires extended-gate field-effect transistor as pH sensor. Thin Solid Films 2013;529:173–6.
[82] Labrador RH, Soto J, Martínez-Máñez R, Coll C, Benito A, Ibáñez J, et al. An electrochemical characterization of thick-film electrodes based on RuO_2-containing resistive pastes. J Electroanal Chem 2007;611:175–80.
[83] Chou JC, Wang YF. Preparation and study on the drift and hysteresis properties of the tin oxide gate ISFET by the sol–gel method. Sens Actuat, B 2002;86:58–62.
[84] Pocrifka LA, Gonçalves C, Grossi P, Colpa PC, Pereira EC. Development of RuO_2–TiO_2 (70–30)mol% for pH measurements. Sens Actuat, B 2006;113:1012–6.
[85] da Silva GM, Lemos SG, Pocrifka LA, Marreto PD, Rosario AV, Pereira EC. Development of low-cost metal oxide pH electrodes based on the polymeric precursor method. Anal Chim Acta 2008;616:36–41.
[86] Cané C, Gràcia I, Merlos A. Microtechnologies for PH ISFET chemical sensors. Microelectron J 1997;28:389–405.
[87] Pijanowska DG, Torbicz W. pH-ISFET based urea biosensor. Sens Actuat, B 1997;44:370–6.
[88] Bergveld P. Development of an ion-sensitive solid-state device for neurophysiological measurements. IEEE Trans Biomed Eng 1970;BME-17:70–1.
[89] Gou P, Kraut ND, Feigel IM, Bai H, Morgan GJ, Chen Y, et al. Carbon nanotube chemiresistor for wireless pH sensing. Sci Rep 2014;4:4468.
[90] Lei N, Li P, Xue W, Xu J. Simple graphene chemiresistors as pH sensors: fabrication and characterization. Meas Sci Technol 2011;22:107002.
[91] Chaisiwamongkhol K, Batchelor-McAuley C, Compton RG. Optimising amperometric pH sensing in blood samples: an iridium oxide electrode for blood pH sensing. Analyst 2019;144:1386–93.
[92] Manjakkal L, Djurdjic E, Cvejin K, Kulawik J, Zaraska K, Szwagierczak D. Electrochemical impedance spectroscopic analysis of RuO2 based thick film pH sensors. Electrochim Acta 2015;168:246–55.
[93] Manjakkal L, Cvejin K, Kulawik J, Zaraska K, Socha RP, Szwagierczak D. X-ray photoelectron spectroscopic and electrochemical impedance spectroscopic analysis of RuO_2-Ta_2O_5 thick film pH sensors. Anal Chim Acta 2016;931:47–56.
[94] Manjakkal L, Cvejin K, Kulawik J, Zaraska K, Szwagierczak D. A comparative study of potentiometric and conductimetric thick film pH sensors made of RuO_2 pastes. Sens Lett 2014;12:1645–50.
[95] Manjakkal L, Cvejin K, Kulawik J, Zaraska K, Szwagierczak D. Electrochemical interdigitated conductimetric ph sensor based on RuO_2 thick film sensitive layer. 2014 International Conference and Exposition on Electrical and Power Engineering (EPE). 2014. p. 797–800.
[96] Bohnke C, Fourquet JL. Impedance spectroscopy on pH-sensors with lithium lanthanum titanate sensitive material. Electrochim Acta 2003;48:1869–78.
[97] Manjakkal L, Vilouras A, Dahiya R. Screen printed thick film reference electrodes for electrochemical sensing. IEEE Sens J 2018;18:7779–85.
[98] Manjakkal L, Pascual CL, Dahiya R. Electrochemical sensors with screen printed Ag|AgCl|KCl reference electrodes. 2017 IEEE SENSORS2017. p. 1-3.
[99] Sophocleous M, Atkinson JK. A review of screen-printed silver/silver chloride (Ag/AgCl) reference electrodes potentially suitable for environmental potentiometric sensors. Sens Actuat, A 2017;267:106–20.
[100] Tymecki Ł, Zwierkowska E, Koncki R. Screen-printed reference electrodes for potentiometric measurements. Anal Chim Acta 2004;526:3–11.
[101] Manjakkal L, Synkiewicz B, Zaraska K, Cvejin K, Kulawik J, Szwagierczak D. Development and characterization of miniaturized LTCC pH sensors with RuO2 based sensing electrodes. Sens Actuat, B 2016;223:641–9.
[102] Manjakkal L, Cvejin K, Kulawik J, Zaraska K, Szwagierczak D, Stojanovic G. Sensing mechanism of RuO2–SnO2 thick film pH sensors studied by potentiometric method and electrochemical impedance spectroscopy. J Electroanal Chem 2015;759:82–90.
[103] Manjakkal L, Shakthivel D, Dahiya R. Flexible printed reference electrodes for electrochemical applications. Adv Mater Technol 2018;3:1800252.
[104] Cranny AWJ, Atkinson JK. Thick film silver-silver chloride reference electrodes. Meas Sci Technol 1998;9:1557–65.
[105] Sun X, Wang M. Fabrication and characterization of planar reference electrode for on-chip electroanalysis. Electrochim Acta 2006;52:427–33.
[106] Vasudev A, Kaushik A, Jones K, Bhansali S. Prospects of low temperature co-fired ceramic (LTCC) based microfluidic systems for point-of-care biosensing and environmental sensing. Microfluid Nanofluid 2013;14:683–702.
[107] Tsung-Hsien L, Kaiser WJ, Pottie GJ. Integrated low-power communication system design for wireless sensor networks. IEEE Commun Mag 2004;42:142–50.
[108] Bandodkar AJ, Wang J. Non-invasive wearable electrochemical sensors: a review. Trends Biotechnol 2014;32:363–71.
[109] Gill E, Arshak K, Arshak A, Korostynska O. Mixed metal oxide films as pH sensing materials. Microsyst Technol 2008;14:499–507.
[110] Antohe VA, Radu A, Mátéfi-Tempfli S, Piraux L. Circuit modeling on polyaniline functionalized nanowire-templated micro-interdigital capacitors for pH sensing. IEEE Trans Nanotechnol 2011;10:1314–20.
[111] Arshak K, Gill E, Arshak A, Korostynska O. Investigation of tin oxides as sensing layers in conductimetric interdigitated pH sensors. Sens Actuat, B 2007;127:42–53.
[112] Jaffrezic-Renault N, Dzyadevych SV. Conductometric microbiosensors for environmental monitoring. Sensors 2008;8:2569–88.
[113] Varshney M, Li Y. Interdigitated array microelectrodes based impedance biosensors for detection of bacterial cells. Biosens Bioelectron 2009;24:2951–60.
[114] Frantzen A, Scheidtmann J, Frenzer G, Maier WF, Jockel J, Brinz T, et al. High-throughput method for the impedance spectroscopic characterization of resistive gas sensors. Angew Chem Int Ed 2004;43:752–4.
[115] Mamishev AV, Sundara-Rajan K, Fumin Y, Yanqing D, Zahn M. Interdigital sensors and transducers. Proc IEEE 2004;92:808–45.
[116] Cvejin K, Manjakkal L, Kulawik J, Zaraska K, Szwagierczak D. Planar impedancemetric NO sensor with thick film mixed dy-based oxides sensing electrodes. 2014 International Conference and Exposition on Electrical and Power Engineering (EPE). 2014. p. 821–4.
[117] Huet F. A review of impedance measurements for determination of the state-of-charge or state-of-health of secondary batteries. J Power Sources 1998;70:59–69.
[118] Manjakkal L, Navaraj WT, Núñez CG, Dahiya R. Graphene-graphite polyurethane composite based high-energy density flexible supercapacitors. Adv Sci

2019;6:1802251.
[119] Pejcic B, De Marco R. Impedance spectroscopy: over 35 years of electrochemical sensor optimization. Electrochim Acta 2006;51:6217–29.
[120] Lasia A. Electrochemical Impedance Spectroscopy and its Applications. In: Conway BE, Bockris JOM, White RE, editors. Modern Aspects of Electrochemistry. Boston, MA: Springer, US; 2002. p. 143–248.
[121] Lvovich VF. Impedance spectroscopy: applications to electrochemical and dielectric phenomena. John Wiley & Sons; 2012.
[122] Lee YT, Lee E, Lee JM, Lee W. Micro-sized pH sensors based on patterned Pd structures using an electrolysis method. Curr Appl Phys 2009;9:e218–21.
[123] Lee WS, Park Y-S, Cho Y-K. Hierarchically structured suspended TiO_2 nanofibers for use in UV and pH sensor devices. ACS Appl Mater Interfaces 2014;6:12189–95.
[124] Bergveld P. Thirty years of ISFETOLOGY: what happened in the past 30 years and what may happen in the next 30 years. Sens Actuat, B 2003;88:1–20.
[125] Liao H-K, Chi L-L, Chou J-C, Chung W-Y, Sun T-P, Hsiung S-K. Study on pHpzc and surface potential of tin oxide gate ISFET. Mater Chem Phys 1999;59:6–11.
[126] Nakazato K. An integrated ISFET sensor array. Sensors 2009;9:8831–51.
[127] Lee C-S, Kim SK, Kim M. Ion-sensitive field-effect transistor for biological sensing. Sensors 2009;9:7111–31.
[128] Van der Spiegel J, Lauks I, Chan P, Babic D. The extended gate chemically sensitive field effect transistor as multi-species microprobe. Sensors Actuat 1983;4:291–8.
[129] Guerra EM, Silva GR, Mulato M. Extended gate field effect transistor using V_2O_5 xerogel sensing membrane by sol–gel method. Solid State Sci 2009;11:456–60.
[130] Campos RdC, Cestarolli DT, Mulato M, Guerra EM. Comparative sensibility study of WO_3 ph sensor using EGFET and ciclic voltammetry. Mater Res 2015;18:15–9.
[131] Hung S-C, Cheng N-J, Yang C-F, Lo Y-P. Investigation of extended-gate field-effect transistor pH sensors based on different-temperature-annealed bi-layer MWCNTs-In_2O_3 films. Nanoscale Res Lett 2014;9:502.
[132] Yao PC, Lee MC, Chiang JL. Annealing effect of sol-gel TiO2 THIN FILM on pH-EGFET sensor. 2014 International Symposium on Computer Consumer and Control. 2014. p. 577–80.
[133] Yin L-T, Chou J-C, Chung W-Y, Sun T-P, Hsiung S-K. Separate structure extended gate H+-ion sensitive field effect transistor on a glass substrate. Sens Actuat, B 2000;71:106–11.
[134] Ahmed Ali AM, Ahmed NM, Mohammad SM, Sabah FA, Kabaa E, Alsadig A, et al. Effect of gamma irradiation dose on the structure and pH sensitivity of ITO thin films in extended gate field effect transistor. Results Phys 2019;12:615–22.
[135] Mokhtarifar N, Goldschmidtboeing F, Woias P. Low-cost EGFET-based pH-sensor using encapsulated ITO/PET-electrodes. 2018 IEEE International Instrumentation and Measurement Technology Conference (I2MTC). 2018. p. 1–5.
[136] Wu Y, Wu S, Lin C. High performance EGFET-based pH sensor utilizing low-cost industrial-grade touch panel film as the gate structure. IEEE Sens J 2015;15:6279–86.
[137] Pyo J-Y, Cho W-J. High-performance SEGISFET pH sensor using the structure of double-gate a-IGZO TFTs with engineered gate oxides. Semicond Sci Technol 2017;32:035015.
[138] Yang J, Kwak TJ, Zhang X, McClain R, Chang W-J, Gunasekaran S. Digital pH test strips for in-field pH monitoring using iridium oxide-reduced graphene oxide hybrid thin films. ACS Sensors 2016;1:1235–43.
[139] McMurray HN, Douglas P, Abbot D. Novel thick-film pH sensors based on ruthenium dioxide-glass composites. Sens Actuat, B 1995;28:9–15.
[140] Buck RP, Lindner E. Recommendations for nomenclature of ionselective electrodes (IUPAC Recommendations 1994). Pure Appl Chem 1994:2527.
[141] Bousse L, Bergveld P. The role of buried OH sites in the response mechanism of inorganic-gate pH-sensitive ISFETs. Sensors Actuat 1984;6:65–78.
[142] Schöning MJ, Brinkmann D, Rolka D, Demuth C, Poghossian A. CIP (cleaning-in-place) suitable "non-glass" pH sensor based on a Ta_2O_5-gate EIS structure. Sens Actuat, B 2005;111–112:423–9.
[143] Chiang J-L, Jan S-S, Chou J-C, Chen Y-C. Study on the temperature effect, hysteresis and drift of pH-ISFET devices based on amorphous tungsten oxide. Sens Actuat, B 2001;76:624–8.
[144] Chou J, Chen C. Fabrication and application of ruthenium-doped titanium dioxide films as electrode material for ion-sensitive extended-gate FETs. IEEE Sens J 2009;9:277–84.
[145] Tsai C-N, Chou J-C, Sun T-P, Hsiung S-K. Study on the sensing characteristics and hysteresis effect of the tin oxide pH electrode. Sens Actuat, B 2005;108:877–82.
[146] Trasatti S. Physical electrochemistry of ceramic oxides. Electrochim Acta 1991;36:225–41.
[147] Mihell JA, Atkinson JK. Planar thick-film pH electrodes based on ruthenium dioxide hydrate. Sens Actuat, B 1998;48:505–11.
[148] Al-Hilli S, Willander M. The pH response and sensing mechanism of n-type ZnO/electrolyte interfaces. Sensors 2009;9:7445–80.
[149] Yates DE, Levine S, Healy TW. Site-binding model of the electrical double layer at the oxide/water interface. J Chem Soc, Faraday Trans 1 F 1974;70:1807–18.
[150] Kurzweil P. Precious metal oxides for electrochemical energy converters: pseudocapacitance and pH dependence of redox processes. J Power Sources 2009;190:189–200.
[151] Kosmulski M. The pH-dependent surface charging and the points of zero charge. J Colloid Interface Sci 2002;253:77–87.
[152] Tombácz E. pH-dependent surface charging of metal oxides. Periodica Polytech, Chem Eng 2009;53:77–86.
[153] Wu Z-S, Wang D-W, Ren W, Zhao J, Zhou G, Li F, et al. Anchoring hydrous RuO_2 on graphene sheets for high-performance electrochemical capacitors. Adv Funct Mater 2010;20:3595–602.
[154] Lonsdale W, Shylendra SP, Brouwer S, Wajrak M, Alameh K. Application of ruthenium oxide pH sensitive electrode to samples with high redox interference. Sens Actuat, B 2018;273:1222–5.
[155] Manjakkal L, Cvejin K, Kulawik J, Zaraska K, Szwagierczak D. A low-cost pH sensor based on RuO_2 resistor material. Nano Hybrids 2013;5:1–15.
[156] Ribeiro J, Moats MS, De Andrade AR. Morphological and electrochemical investigation of RuO_2–Ta_2O_5 oxide films prepared by the Pechini-Adams method. J Appl Electrochem 2008;38:767–75.
[157] Ribeiro J, Purgato FL, Léger JM, de Andrade AR. Application of Ti/RuO2–Ta2O5 electrodes in the electrooxidation of ethanol and derivants: reactivity versus electrocatalytic efficiency. Electrochim Acta 2008;53:7845–51.
[158] Cardarelli F, Taxil P, Savall A, Comninellis C, Manoli G, Leclerc O. Preparation of oxygen evolving electrodes with long service life under extreme conditions. J Appl Electrochem 1998;28:245–50.
[159] Zhuiykov S. Development of ceramic electrochemical sensor based on $Bi_2Ru_2O_{7+x} - RuO_2$ sub-micron oxide sensing electrode for water quality monitoring. Ceram Int 2010;36:2407–13.
[160] Koncki R, Mascini M. Screen-printed ruthenium dioxide electrodes for pH measurements. Anal Chim Acta 1997;351:143–9.
[161] Katsube T, Lauks I, Zemel JN. pH-sensitive sputtered iridium oxide films. Sensors Actuat 1981;2:399–410.
[162] Kreider K. Iridium oxide thin-film stability in high-temperature corrosive solutions. Sens Actuat, B 1991;5:165–9.
[163] Korotcov AV, Huang Y-S, Tiong K-K, Tsai D-S. Raman scattering characterization of well-aligned RuO2 and IrO2 nanocrystals. J Raman Spectrosc 2007;38:737–49.
[164] Cai Z. Mechanism of electrochemical evolution of chlorine and oxygen at Ti/SnO_2-IrO_2 anode. Prog Nat Sci 2005;15:76–81.
[165] Kuznetsova E, Petrykin V, Sunde S, Krtil P. Selectivity of nanocrystalline IrO_2-based catalysts in parallel chlorine and oxygen evolution. Electrocatalysis 2015;6:198–210.
[166] Nishio K, Tsuchiya T. Electrochromic thin films prepared by sol–gel process. Sol Energy Mater Sol Cells 2001;68:279–93.
[167] Nguyen CM, Huang W, Rao S, Cao H, Tata U, Chiao M, et al. Sol-gel iridium oxide-based pH sensor array on flexible polyimide substrate. IEEE Sens J 2013;13:3857–64.
[168] Pásztor K, Sekiguchi A, Shimo N, Kitamura N, Masuhara H. Iridium oxide-based microelectrochemical transistors for pH sensing. Sens Actuat, B 1993;12:225–30.
[169] Kinlen PJ, Heider JE, Hubbard DE. A solid-state pH sensor based on a Nafion-coated iridium oxide indicator electrode and a polymer-based silver chloride

reference electrode. Sens Actuat, B 1994;22:13–25.
[170] Chung H-J, Sulkin MS, Kim J-S, Goudeseune C, Chao H-Y, Song JW, et al. Stretchable, multiplexed pH sensors with demonstrations on rabbit and human hearts undergoing ischemia. Adv Healthcare Mater 2014;3:59–68.
[171] Zamora ML, Dominguez JM, Trujillo RM, Goy CB, Sánchez MA, Madrid RE. Potentiometric textile-based pH sensor. Sens Actuat, B 2018;260:601–8.
[172] Ito Y. Long-term drift mechanism of Ta_2O_5 gate pH-ISFETs. Sens Actuat, B 2000;64:152–5.
[173] Yoshida S, Hara N, Sugimoto K. Development of a wide range pH sensor based on electrolyte-insulator-semiconductor structure with corrosion-resistant Al_2O_3-Ta_2O_5 and Al_2O_3-ZrO_2 double-oxide thin films. J Electrochem Soc 2004;151:H53–8.
[174] Barsan N, Schweizer-Berberich M, Göpel W. Fundamental and practical aspects in the design of nanoscaled SnO2 gas sensors: a status report. Fresenius' J Anal Chem 1999;365:287–304.
[175] Kohl D. Function and applications of gas sensors. J Phys D Appl Phys 2001;34:R125.
[176] Pan C-W, Chou J-C, Sun T-P, Hsiung S-K. Development of the tin oxide pH electrode by the sputtering method. Sens Actuat, B 2005;108:863–9.
[177] Liao H-K, Chou J-C, Chung W-Y, Sun T-P, Hsiung S-K. Study of amorphous tin oxide thin films for ISFET applications. Sens Actuat, B 1998;50:104–9.
[178] Chin Y-L, Chou J-C, Sun T-P, Chung W-Y, Hsiung S-K. A novel pH sensitive ISFET with on chip temperature sensing using CMOS standard process. Sens Actuat, B 2001;76:582–93.
[179] Pan C-W, Chou J-C, Sun T-P, Hsiung S-K. Development of the real-time pH sensing system for array sensors. Sens Actuat, B 2005;108:870–6.
[180] Cheng Y, Xiong P, Yun CS, Strouse GF, Zheng JP, Yang RS, et al. Mechanism and optimization of pH sensing using SnO2 nanobelt field effect transistors. Nano Lett 2008;8:4179–84.
[181] Batista PD, Mulato M, Graeff CFdO, Fernandez FJR. Marques FdC. SnO2 extended gate field-effect transistor as pH sensor. Braz J Phys 2006;36:478–81.
[182] Chen Y, Mun SC, Kim J. A wide range conductometric pH sensor made with titanium dioxide/multiwall carbon nanotube/cellulose hybrid nanocomposite. IEEE Sens J 2013;13:4157–62.
[183] Huang Y-C, Tsai F-S, Wang S-J. Preparation of TiO2 nanowire arrays through hydrothermal growth method and their pH sensing characteristics. Jpn J Appl Phys 2014;53:06JG2.
[184] Simić M, Manjakkal L, Zaraska K, Stojanović GM, Dahiya R. TiO_2-based thick film pH sensor. IEEE Sens J 2017;17:248–55.
[185] Natan MJ, Mallouk TE, Wrighton MS. The pH-sensitive tungsten(VI) oxide-based microelectrochemical transistors. J Phys Chem 1987;91:648–54.
[186] Manjakkal L, Packia Selvam I, Potty SN, Shinde RS. Electrical and optical properties of aluminium doped zinc oxide transparent conducting oxide films prepared by dip coating technique. Microelectr Int 2017;34:1–8.
[187] Rong P, Ren S, Yu Q. Fabrications and applications of ZnO nanomaterials in flexible functional devices-a review. Crit Rev Anal Chem 2018;1–14.
[188] Kang BS, Ren F, Heo YW, Tien LC, Norton DP, Pearton SJ. pH measurements with single ZnO nanorods integrated with a microchannel. Appl Phys Lett 2005;86:112105.
[189] Wei A, Pan L, Huang W. Recent progress in the ZnO nanostructure-based sensors. Mater Sci Eng, B 2011;176:1409–21.
[190] Shakthivel D, Yogeswaran N, Manjakkal L, Dahiya R. Flexible ZnO nanowires-graphene stack by hot lamination method. 2018 IEEE Sensors 2018:1–4.
[191] Batista PD, Mulato M. ZnO extended-gate field-effect transistors as pH sensors. Appl Phys Lett 2005;87:143508.
[192] Chiu Y, Tseng C, Lee C. Nanostructured EGFET pH sensors with surface-passivated ZnO thin-film and nanorod array. IEEE Sens J 2012;12:930–4.
[193] Sakthivel B, Manjakkal L, Nammalvar G. High performance CuO nanorectangles-based room temperature flexible NH3 sensor. IEEE Sens J 2017;17:6529–36.
[194] Ahmad R, Tripathy N, Ahn M-S, Bhat KS, Mahmoudi T, Wang Y, et al. Highly efficient non-enzymatic glucose sensor based on CuO modified vertically-grown ZnO nanorods on electrode. Sci Rep 2017;7:5715.
[195] Rahim A, Rehman ZU, Mir S, Muhammad N, Rehman F, Nawaz MH, et al. A non-enzymatic glucose sensor based on CuO-nanostructure modified carbon ceramic electrode. J Mol Liq 2017;248:425–31.
[196] Jiang L-C, Zhang W-D. A highly sensitive nonenzymatic glucose sensor based on CuO nanoparticles-modified carbon nanotube electrode. Biosens Bioelectron 2010;25:1402–7.
[197] Singh BK, Shaikh A, Badrayyana S, Mohapatra D, Dusane RO, Parida S. Nanoporous gold–copper oxide based all-solid-state micro-supercapacitors. RSC Adv 2016;6:100467–75.
[198] Li Z, Shao M, Zhou L, Zhang R, Zhang C, Han J, et al. A flexible all-solid-state micro-supercapacitor based on hierarchical CuO@layered double hydroxide core–shell nanoarrays. Nano Energy 2016;20:294–304.
[199] Mai YJ, Wang XL, Xiang JY, Qiao YQ, Zhang D, Gu CD, et al. CuO/graphene composite as anode materials for lithium-ion batteries. Electrochim Acta 2011;56:2306–11.
[200] Hong Q, Cao Y, Xu J, Lu H, He J, Sun J-L. Self-powered ultrafast broadband photodetector based on p–n heterojunctions of CuO/Si nanowire array. ACS Appl Mater Interfaces 2014;6:20887–94.
[201] Sun W, Li Y, Ye S, Rao H, Yan W, Peng H, et al. High-performance inverted planar heterojunction perovskite solar cells based on a solution-processed CuOx hole transport layer. Nanoscale 2016;8:10806–13.
[202] Wang G, Huang J, Chen S, Gao Y, Cao D. Preparation and supercapacitance of CuO nanosheet arrays grown on nickel foam. J Power Sources 2011;196:5756–60.
[203] Zhang X, Shi W, Zhu J, Kharistal DJ, Zhao W, Lalia BS, et al. High-power and high-energy-density flexible pseudocapacitor electrodes made from porous CuO nanobelts and single-walled carbon nanotubes. ACS Nano 2011;5:2013–9.
[204] Zhang Q, Zhang K, Xu D, Yang G, Huang H, Nie F, et al. CuO nanostructures: Synthesis, characterization, growth mechanisms, fundamental properties, and applications. Prog Mater Sci 2014;60:208–337.
[205] Heng B, Qing C, Sun D, Wang B, Wang H, Tang Y. Rapid synthesis of CuO nanoribbons and nanoflowers from the same reaction system, and a comparison of their supercapacitor performance. RSC Adv 2013;3:15719–26.
[206] Jiang X, Herricks T, Xia Y. CuO nanowires can be synthesized by heating copper substrates in air. Nano Lett 2002;2:1333–8.
[207] Zaman S, Asif MH, Zainelabdin A, Amin G, Nur O, Willander M. CuO nanoflowers as an electrochemical pH sensor and the effect of pH on the growth. J Electroanal Chem 2011;662:421–5.
[208] Lvov SN, Zhou XY, Ulmer GC, Barnes HL, Macdonald DD, Ulyanov SM, et al. Progress on yttria-stabilized zirconia sensors for hydrothermal pH measurements. Chem Geol 2003;198:141–62.
[209] Macdonald DD, Hettiarachchi S, Lenhart SJ. The thermodynamic viability of yttria-stabilized zirconia pH sensors for high temperature aqueous solutions. J Solut Chem 1988;17:719–32.
[210] Niedrach LW. A new membrane-type pH sensor for use in high temperature-high pressure water. J Electrochem Soc 1980;127:2122–30.
[211] Seneviratne DS, Papangelakis VG, Zhou XY, Lvov SN. Potentiometric pH measurements in acidic sulfate solutions at 250 °C relevant to pressure leaching. Hydrometallurgy 2003;68:131–9.
[212] Betelu S, Polychronopoulou K, Rebholz C, Ignatiadis I. Novel CeO_2-based screen-printed potentiometric electrodes for pH monitoring. Talanta 2011;87:126–35.
[213] Eftekhari A. pH sensor based on deposited film of lead oxide on aluminum substrate electrode. Sens Actuat, B 2003;88:234–8.
[214] Razmi H, Heidari H, Habibi E. pH-sensing properties of PbO_2 thin film electrodeposited on carbon ceramic electrode. J Solid State Electrochem 2008;12:1579–87.
[215] Bohnke C, Duroy H, Fourquet JL. pH sensors with lithium lanthanum titanate sensitive material: applications in food industry. Sens Actuat, B 2003;89:240–7.
[216] Bohnke C, Regrag B, Le Berre F, Fourquet JL, Randrianantoandro N. Comparison of pH sensitivity of lithium lanthanum titanate obtained by sol–gel synthesis and solid state chemistry. Solid State Ionics 2005;176:73–80.
[217] Vijayakumar M, Pham QN, Bohnke C. Lithium lanthanum titanate ceramic as sensitive material for pH sensor: influence of synthesis methods and powder grains size. J Eur Ceram Soc 2005;25:2973–6.
[218] Telli L, Brahimi B, Hammouche A. Study of a pH sensor with MnO_2 and montmorillonite-based solid-state internal reference. Solid State Ionics 2000;128:255–9.
[219] Qingwen L, Yiming W, Guoan L. pH-Response of nanosized MnO_2 prepared with solid state reaction route at room temperature. Sens Actuat, B 1999;59:42–7.
[220] Qingwen L, Guoan L, Youqin S. Response of nanosized cobalt oxide electrodes as pH sensors. Anal Chim Acta 2000;409:137–42.

[221] Hashimoto T, Miwa M, Nasu H, Ishihara A, Nishio Y. pH sensors using 3d-block metal oxide-coated stainless steel electrodes. Electrochim Acta 2016;220:699–704.
[222] Shuk P, Ramanujachary KV, Greenblatt M. New metal-oxide-type pH sensors. Solid State Ionics 1996;86–88:1115–20.
[223] Chou J, Yan S, Liao Y, Lai C, Chen J, Chen H, et al. Characterization of flexible arrayed pH sensor based on nickel oxide films. IEEE Sens J 2018;18:605–12.
[224] Padmanathan N, Shao H, Razeeb KM. Multifunctional nickel phosphate nano/microflakes 3D electrode for electrochemical energy storage, nonenzymatic glucose, and sweat pH sensors. ACS Appl Mater Interfaces 2018;10:8599–610.
[225] Pan T-M, Wang C-W, Mondal S, Pang S-T. Super-Nernstian sensitivity in microfabricated electrochemical pH sensor based on CeTixOy film for biofluid monitoring. Electrochim Acta 2018;261:482–90.
[226] Mohammad-Rezaei R, Soroodian S, Esmaeili G. Manganese oxide nanoparticles electrodeposited on graphenized pencil lead electrode as a sensitive miniaturized pH sensor. J Mater Sci: Mater Electron 2019;30:1998–2005.
[227] Manjakkal L, Cvejin K, Kulawik J, Zaraska K, Szwagierczak D. The effect of sheet resistivity and storage conditions on sensitivity of RuO_2 based pH sensors. Key Eng Mater 2014;605:457–60.
[228] Karimi Shervedani R, Zare Mehrdjardi HR, Kazemi Ghahfarokhi SH. Electrochemical characterization and application of Ni-RuO2 as a pH sensor for determination of petroleum oil acid number. J Iran Chem Soc 2007;4:221–8.
[229] Teixeira MFS, Ramos LA, Fatibello-Filho O, Cavalheiro ÉTG. PbO_2-based graphite–epoxy electrode for potentiometric determination of acids and bases in aqueous and aqueous–ethanolic media. Fresenius' J Anal Chem 2001;370:383–6.
[230] Saravanakumar B, Soyoon S, Kim S-J. Self-powered pH sensor based on a flexible organic-inorganic hybrid composite nanogenerator. ACS Appl Mater Interfaces 2014;6:13716–23.
[231] Kim TY, Hong SA, Yang S. A solid-state thin-film Ag/AgCl reference electrode coated with graphene oxide and its use in a pH sensor. Sensors 2015;15:6469–82.
[232] Shitanda I, Komoda M, Hoshi Y, Itagaki M. An instantly usable paper-based screen-printed solid-state KCl/Ag/AgCl reference electrode with long-term stability. Analyst 2015;140:6481–4.
[233] Cvejin K, Manjakkal L, Kulawik J, Zaraska K, Szwagierczak D. Synthesis of perovskite Sr doped lanthanide cobaltites and ferrites and application for oxygen sensors: a comparative study. Key Eng Mater 2014;605:483–6.
[234] Cvejin K, Manjakkal L, Kulawik J, Zaraska K, Szwagierczak D. Planar impedancemetric NO sensor with thick film perovskite electrodes based on samarium cobaltite. Electroanalysis 2015;27:760–9.
[235] Cvejin K, Śliwa M, Manjakkal L, Kulawik J, Stojanović G, Szwagierczak D. Impedancemetric NO sensor based on YSZ/perovskite neodymium cobaltite operating at high temperatures. Sens Actuat, B 2016;228:612–24.
[236] Mariana S, Anatolie I, Manjakkal L, Villalba JFB. Design of data acquisition system for environmental sensors manufactured in LTCC technology. 2014 International Conference and Exposition on Electrical and Power Engineering (EPE). 2014. p. 845–8.
[237] Wang N, Zhang N, Wang M. Wireless sensors in agriculture and food industry—recent development and future perspective. Comput Electron Agric 2006;50:1–14.
[238] Li S, Simonian A, Chin BA. Sensors for agriculture and the food industry. Electrochem Soc Interface 2010;19:41–6.
[239] Nakata S, Shiomi M, Fujita Y, Arie T, Akita S, Takei K. A wearable pH sensor with high sensitivity based on a flexible charge-coupled device. Nat Electron 2018;1:596–603.
[240] Schreml S, Szeimies R-M, Karrer S, Heinlin J, Landthaler M, Babilas P. The impact of the pH value on skin integrity and cutaneous wound healing. J Eur Acad Dermatol Venereol 2010;24:373–8.
[241] Lambers H, Piessens S, Bloem A, Pronk H, Finkel P. Natural skin surface pH is on average below 5, which is beneficial for its resident flora. Int J Cosmet Sci 2006;28:359–70.
[242] Weber J, Kumar A, Kumar A, Bhansali S. Novel lactate and pH biosensor for skin and sweat analysis based on single walled carbon nanotubes. Sens Actuat, B 2006;117:308–13.
[243] Curto VF, Coyle S, Byrne R, Angelov N, Diamond D, Benito-Lopez F. Concept and development of an autonomous wearable micro-fluidic platform for real time pH sweat analysis. Sens Actuat, B 2012;175:263–70.
[244] Emaminejad S, Gao W, Wu E, Davies ZA, Yin Yin Nyein H, Challa S, et al. Autonomous sweat extraction and analysis applied to cystic fibrosis and glucose monitoring using a fully integrated wearable platform. Proceedings of the National Academy of Sciences. 2017. p. 4625–30.
[245] Gao W, Emaminejad S, Nyein HYY, Challa S, Chen K, Peck A, et al. Fully integrated wearable sensor arrays for multiplexed in situ perspiration analysis. Nature 2016;529:509.
[246] Zhang H, Yang Y, Su Y, Chen J, Hu C, Wu Z, et al. Triboelectric nanogenerator as self-powered active sensors for detecting liquid/gaseous water/ethanol. Nano Energy 2013;2:693–701.
[247] Nie C, Frijns A, Zevenbergen M. Toonder Jd. An integrated flex-microfluidic-Si chip device towards sweat sensing applications. Sens Actuat, B 2016;227:427–37.
[248] Chou J, Lin C, Liao Y, Chen J, Tsai Y, Chen J, et al. Data fusion and fault diagnosis for flexible arrayed pH sensor measurement system based on LabVIEW. IEEE Sens J 2014;14:1405–11.
[249] Lue C-E, Wang IS, Huang C-H, Shiao Y-T, Wang H-C, Yang C-M, et al. pH sensing reliability of flexible ITO/PET electrodes on EGFETs prepared by a roll-to-roll process. Microelectron Reliab 2012;52:1651–4.
[250] Lin J-C, Huang B-R, Yang Y-K. IGZO nanoparticle-modified silicon nanowires as extended-gate field-effect transistor pH sensors. Sens Actuat, B 2013;184:27–32.
[251] Kim M-G, Kanatzidis MG, Facchetti A, Marks TJ. Low-temperature fabrication of high-performance metal oxide thin-film electronics via combustion processing. Nat Mater 2011;10:382.
[252] Núñez CG, Navaraj WT, Polat EO, Dahiya R. Energy-autonomous, flexible, and transparent tactile skin. Adv Funct Mater 2017;27:1606287.
[253] García Núñez C, Navaraj WT, Liu F, Shakthivel D, Dahiya R. Large-area self-assembly of silica microspheres/nanospheres by temperature-assisted dip-coating. ACS Appl Mater Interfaces 2018;10:3058–68.
[254] Núñez CG, Manjakkal L, Liu F, Dahiya R. Contact-printing of zinc oxide nanowires for chemical sensing applications. 2018 IEEE Sensors 2018:1–4.
[255] Zhang R, Zhang X, Hu S. High temperature and pressure chemical sensors based on Zr/ZrO_2 electrode prepared by nanostructured ZrO_2 film at Zr wire. Sens Actuat, B 2010;149:143–54.
[256] Yu J, Khalil M, Liu N, Lee R. Iridium oxide-based chemical sensor for in situ pH measurement of oilfield-produced water under subsurface conditions. Ionics 2015;21:855–61.
[257] Manjakkal L, Nikbakhtnasrabadi F, Dahiya R. Energy autonomous sensors for water quality monitoring. 2018 IEEE Sensors 2018:1–4.
[258] Ryuh Y-S, Yang G-H, Liu J, Hu H. A school of robotic fish for mariculture monitoring in the sea coast. J Bionic Eng 2015;12:37–46.
[259] Valada A, Velagapudi P, Kannan B, Tomaszewski C, Kantor G, Scerri P. Development of a Low Cost Multi-Robot Autonomous Marine Surface Platform. In: Yoshida K, Tadokoro S, editors. Field and Service Robotics: Results of the 8th International Conference. Springer, Berlin Heidelberg: Berlin, Heidelberg; 2014. p. 643–58.